JOINT ICI CANCELLATION, CHANNEL ESTIMATION AND ERROR CORRECTION IN ITERATIVE FASHION

by

Zeeshan Sabir

Thesis submitted to the faculty of Electrical Engineering Department Military College of Signals, National University of Sciences and Technology, Rawalpindi in partial fulfillment for the requirements of a Masters Degree in Electrical Engineering

NOVEMBER 2009

ABSTRACT

JOINT ICI CANCELLATION, CHANNEL ESTIMATION AND ERROR CORRECTION IN ITERATIVE FASHION

By

Zeeshan Sabir

The rapid advancement in the field of wireless communications that has been expedited by the commercial demand for better services has led to the application of wireless systems in many fields of life including education, military, medical and many real time services. A number of these services demand a high data rate for the applications to run. OFDM is a promising technique that can provide this high data rate by efficiently utilizing the available bandwidth. The problem with this technique is the high Inter-Carrier Interference that occurs due to the disturbance of orthogonality between the subcarriers of an OFDM symbol during the course of transmission. This requires a better channel estimation strategy. Alongwith this, despite the fact that most of the emerging wireless standards such as 802.11n (Wi-Fi) and 802.16e (WiMax) use OFDM technique for increased spectral efficiency and improvement of performance, very little attention has been paid to the use of efficient error correcting Turbo codes in

these systems. The BER of the published work is still not better than 10^{-3} at affordable SNR for lower modulation schemes.

In this research we have applied Frequency-domain equalization technique for suppressing ICI in the OFDM system and have integrated Turbo Codes in the resulting system for error correction. We have worked on the design of an efficient encoder and decoder. The decoder uses an iterative mechanism for decoding the received bits that is based on Maximum *a posteriori* algorithm. The error reduction achieved by the iterative mechanism of the Turbo Decoder improves the overall coding gain of the system. Results have been achieved for a number of lower order modulation schemes through MATLAB simulation with and without Turbo Codes implementation and with the application of Frequency-domain equalization strategy.

DEDICATION

All praise and thanks to almighty Allah, the most gracious and the most merciful, Master of the Day of Judgment. Guide us with courage and right path, path of those to whom You have bestowed your blessings.

Dedicated to my Parents and wife, whose selfless cooperation made it possible for me to complete this work

ACKNOWLEDGEMENT

I would like to thanks my supervisor Lt. Col. Dr. Muhammad Arif Wahla, Head of Information Security Department, Military College of Signals, NUST for his continuous encouragement and necessary guidance. I'll always remain indebted for his extraordinary and wholehearted support.

I am also thankful to my guidance committee members Maj. Fazal Ahmed, Maj. Dr. Adnan Ahmed Khan and Lec. Khurram Shahzad for their able guidance throughout the process. Besides I owe my gratitude to Col. Atiq Ahmad, HOD EE Deptt. who facilitated me at every step in enhancing my research related activities.

TABLE OF CONTENTS

LIST OF FIGURES

LIST OF ABBREVIATIONS

OFDM	Orthogonal Frequency Division Multiplexing
WLAN	Wireless Local Area Network
WiMAX	Wide Interoperability of Microwave Access
WiFi	Wireless Fidelity
FFT	Fast Fourier Transform
ICI	Inter Carrier Interference
ISI	Inter Symbol Interference
IBI	Inter Block Interference
AWGN	Additive White Gaussian Noise
BER	Bit Error Rate
FDM	Frequency Division Multiplexing
MCM	Multi-Carrier Modulation
DAB	Digital Audio Broadcasting
DVB	Digital Video Broadcasting
CFO	Channel Frequency Offset
CP	Cyclic Prefix

PCC	Polynomial Cancellation Coded
PAPR	Peak to Average Power Ratio
FEC	Forward Error Correction
RSC	Recursive Systematic Convolutional
MAP	Maximum *A Posteriori*
SOVA	Soft Output Viterbi Algorithm
LOS	Line Of Sight
MIMO	Multiple Input Multiple Output
SISO	Single Input Single Output
QOS	Quality of Service

Chapter-1

INTRODUCTION

1.1 Motivation

Wireless communication is an emerging field, which has seen colossal growth in the last several years and this rapid growth has resulted in the development of high data rate communications e.g. Wireless LANs, WLANs (802.11 a/g), WiMax (802.16e) and WiFi (802.11n). The motive behind the development of all these technologies is to achieve high data rate with limited bandwidth and power consumption to enable the customers to enjoy the services of high data rate applications like Multimedia streaming, Digital Audio/Video Broadcasting etc.

Orthogonal Frequency Division Multiplexing (OFDM) is a technique that transforms a frequency-selective wide-band channel into a cluster of non-selective narrowband channels, which makes it efficient in the environment of large delay spreads by maintaining orthogonality between the subcarriers in both the frequency and time domains. Moreover, the nifty introduction of cyclic prefix in the final stage at the transmitter reduces the complexity to only FFT processing and one tap equalization at the receiver is sufficient to reduce the carrier interferences.

Though OFDM is attractive for high data rate wireless transmission, it is also sensitive to synchronization errors (symbol time and frequency offset). Hence reliable transmission schemes are needed **[1].** Although OFDM based commercial WLANs (802.11a/g) support peak data rate of 54Mbps at most **[2],** the signal of OFDM based multicarrier transmission is prone to different type of impairments that are introduced due to fading channels. Inter Carrier Interference (ICI) and Inter Symbol/Block Interference (ISI/IBI) are worth mentioning. And it was also the basic motive behind our thesis to develop a scheme that can reduce these interferences in the OFDM in the most efficient manner.

Since there introduction in 1993, Turbo codes have gained a lot of attention from the research community, all around the globe. The iterative error correcting capability of these codes, enables the user to maintain the reliability of the information during transmitting it over fading channels. The basic motive behind our thesis is to propose a communication system based on OFDM technique that can exploit the error correcting capability of Turbo codes along with estimating the channel and reducing the ICI and ISI effects in the most efficient manner and with minimum complexity.

1.2 Problem Statement

In most of the practical environments, there is a relative motion between the transmitter and receiver. Due to these relative motions, Doppler frequencies are generated which disturb the orthogonality of the subcarriers in OFDM based systems by mismatching peaks of one subcarrier with the nulls of the other subcarriers (pl. refer sec. 2.3). It generates Inter-Carrier-Interference (ICI) amongst the subcarriers which add to the impairments in the transmitted data streams. Thus, due to sensitivity of OFDM System to the Doppler frequencies in the fading environment, which disturbs the orthogonality of subcarriers, there is a need of ICI cancellation and channel estimation of the OFDM System.

Alongwith this, BER performance of the present systems is in the range of 10e-2 to 10e-3 which is not considered ideal for many sensitive applications. Thus some proper error correcting codes should be integrated in the present systems, that can bring down the BER to the range of 10e-4. Turbo codes are the best option in this context because of significant power efficiency in AWGN and flat-fading channels for fairly low BER and there flexibility of Deign tradeoffs appropriate for delivery of multimedia services mentioned in Sec. 1.1.

1.3 Thesis Objective

The field of Channel estimation and ICI cancellation is still a hot, active and open area of research because of increasing demand for high data rate at low power consumption and BER. Because of transmission of data at low power, the fading channel impairments in the data become very high and efficient channel estimation is indispensable.

Therefore, the basic objective of the thesis is to devise a communication system based on OFDM technique that is capable of doing channel estimation, mitigating ICI and error correction in the most efficient manner with minimum power consumption and data overhead. For this purpose frequency-domain equalization technique is implemented in conjunction with error correcting Turbo codes to bring down the BER of the published work form its present range to 10e-4 at affordable SNR.

1.4 Thesis Organization

The thesis is organized as follows:

*Chapter-1*gives an introduction to the work being carried out under this project. This chapter also contains the basic information about the thesis like the problem statement that is addressed and basic objectives of the thesis.

Chapter-2 provides an introduction to the Orthogonal Frequency Division Multiplexing(OFDM). This chapter contains introduction to all the features

of OFDM that are used or addressed in this thesis like ISI, ICI and the principles governing orthogonality of subcarriers in OFDM etc.

Chapter-3 presents an introduction to Turbo codes. This chapter gives a brief but precise description of different types of Convolutional Encoders, systematic and non-systematic encoders, recursive, non-recursive encoders, there advantages/disadvantages and uses in different scenarios. Second portion of this chapter is dedicated to the Turbo decoders and different decoding algorithms. MAP decoding algorithm used in our work is explained with sufficient details with an introduction to SOVA algorithm alongwith there mathematical descriptions.

Chapter-4 puts a light on the different strategies that are used for channel estimation and equalization for OFDM system. The first portion of this chapter is dedicated to the different types of wireless channels. Then a discussion on fading and its types is given, followed by an explanation of different types of channel estimation and equalization strategies. Both the channel estimation methods i.e. block type and comb-type pilot assisted channel estimation strategies are discussed in sufficient detail in this chapter. At the end of the chapter, three algorithms i.e. Zero forcing, Least Square and Minimum Mean Square Error algorithms are discussed.

Chapter-5 concludes the discussion after giving the implementation details and shows the graphic results of the simulation of the proposed model. The simulation results are given for different environments and channels with/without turbo codes using several modulation schemes. Results conform to the theoretical inferences made in the first four chapters.

Chapter-6 gives overall findings of the research and shows direction for any future work that can be carried out in this field.

Chapter-2

OROTHOGONAL FREQUENCY DIVISION MULTIPLEXING (OFDM)

2.1 Introduction

Orthogonal Frequency Division Multiplexing(OFDM) is a technique of digital communication that splits a large bandwidth into smaller subcarriers for parallel data transfer. Each of this subcarrier (sometimes also called channel) is configured into a narrow bandwidth modulation with each channel operating at a different frequency. The operation at different frequencies makes the subcarriers *orthogonal*. The OFDM technique makes it possible for multiple channels to function within close frequency levels, without compromising the integrity of data transmitted in any one channel. The orthogonality prevents the demodulators from demodulating/sensing other frequencies. The functionality of subcarriers in close frequency levels makes the OFDM technique bandwidth efficient.

2.2 Background of OFDM

The history of OFDM goes back to mid 60s. But the use of Frequency Division Multiplexing (FDM) (predecessor of OFDM) goes back over a century [3], where more than one low rate signal, such as telegraph, was carried over a relatively wide bandwidth channel using a separate carrier

frequency for each signal. OFDM is more robust against frequency-selective fading that causes narrow-band interference. If we are using a single-carrier system, then a single fade or interferer can destroy the whole link, while in the case of a multi-carrier system, only a number of subcarriers will be affected, which can be recovered by the application of proper equalization and error-control coding (*e.g. Turbo Codes*). In the case of multi-carrier communication technique FDM, in order to make possible separation of the signals at the receiver, the carrier frequencies were spaced suitably far apart so that the signal spectra did not overlap. Empty spectral regions called Guard Intervals between the signals assured that they could be separated with readily realizable filters. The resulting spectral efficiency was therefore quite low.

Because of this low spectral efficiency of FDM there was need of a technique that can handle the available bandwidth more efficiently. This idea gave birth to OFDM.

Some early developments regarding OFDM are traced back to 1950s. The concept of using parallel data transfer and frequency-division multiplexing was used in mid 60s [4] when for the first time OFDM was

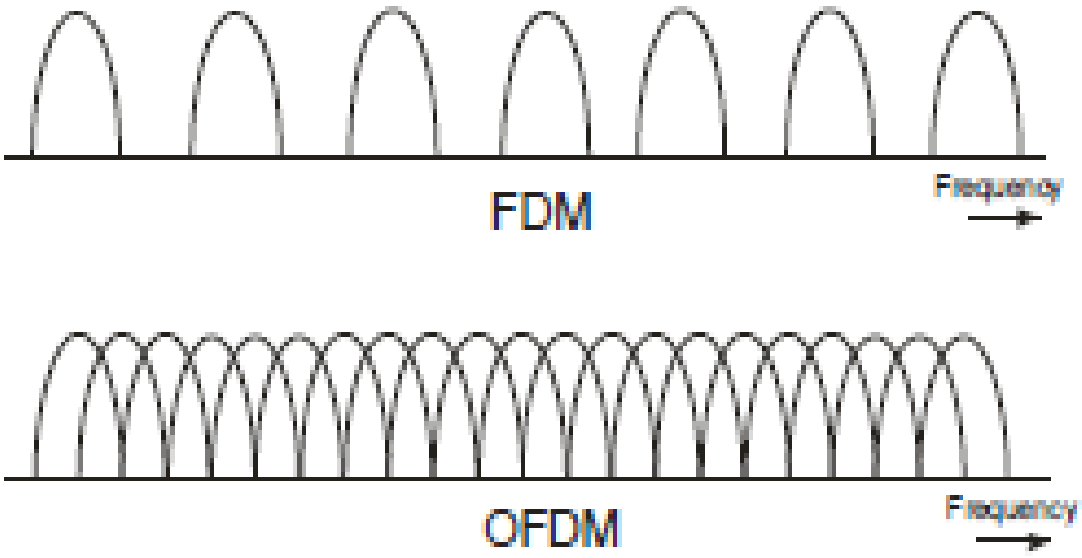

Figure 2.1: A comparison of FDM and OFDM techniques in terms of BW saving

used in several high frequency military systems e.g. KINEPLEX[5], ANDEFT[6] and KATHRYN[7]. A U.S patent regarding OFDM was filed and issued in 1970[8]. Discrete Fourier transform was first applied to the parallel data transmission by Weinstein and Ebert in 1971[9].

The basic concept of OFDM underlies in the fact that the subcarriers overlap in frequency-domain for efficient BW utilization but still don't interfere (ideally). In general 50% bandwidth is saved while using OFDM as compared to FDM[10]. OFDM is an optimal version of Multi-Carrier Modulation(MCM) in the sense that it considers the subcarriers to be perfectly orthogonal.

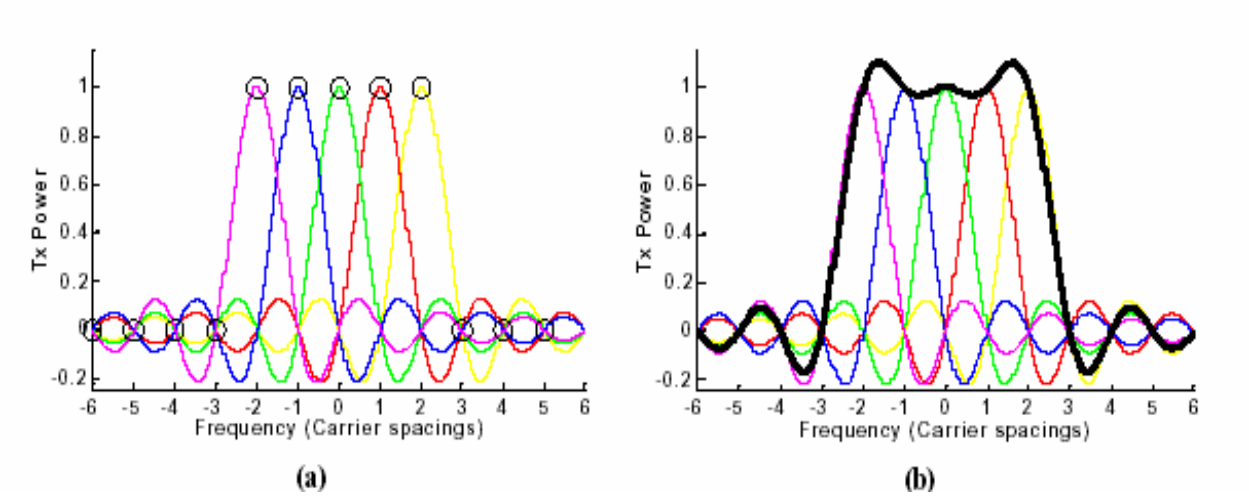

Fig2.2:a. Perfectly Orthogonal OFDM Subcarriers b. An Envelop of Subcarriers

OFDM is used in a variety of techniques like WLAN(802.11(a/g)), WiMax(802.11e), Wi-Fi(802.11n), mobile radio FM channels, Digital Audio Broadcasting(DAB), Digital Video Broadcasting(DVB), Digital High-definition Television (HDTV) broadcasting etc[11][12].

2.3 Principle of Orthogonality

In OFDM the subcarrier frequencies are chosen, such, that the subcarriers are orthogonal to each other. Orthogonality is maintained by the condition that peak of one subcarrier is at the null of other subcarriers as shown in figure 2.2(a). The orthogonality dictates that there is no crosstalk between the subcarrier and thus no guard band is required between the subcarriers as in case of FDM as shown in Fig.2.1. This greatly simplifies the transmitter and receiver design and at the same time adds to the spectral efficiency of

the system. Due to orthogonality, no separate filter is required for each subcarrier. In order to preserve orthogonality, transmitter and receiver should be perfectly synchronized i.e both should have the same modulation frequency and same time-scale for transmission. Secondly if the subcarriers have to be kept orthogonal, there should be no multipath effect. To cater for the multipaths, we use Cyclic Prefix. But perfect synchronization of the transmitter and receive clocks is not possible. Therefore, Channel Frequency Offsets(CFO) are a must in almost all the practical OFDM systems. Another cause of CFO is Doppler effect, which is due to the relative motion between the transmitter and receiver. A typical OFDM subcarrier with and with-out channel frequency offset is shown in fig. 2.3.

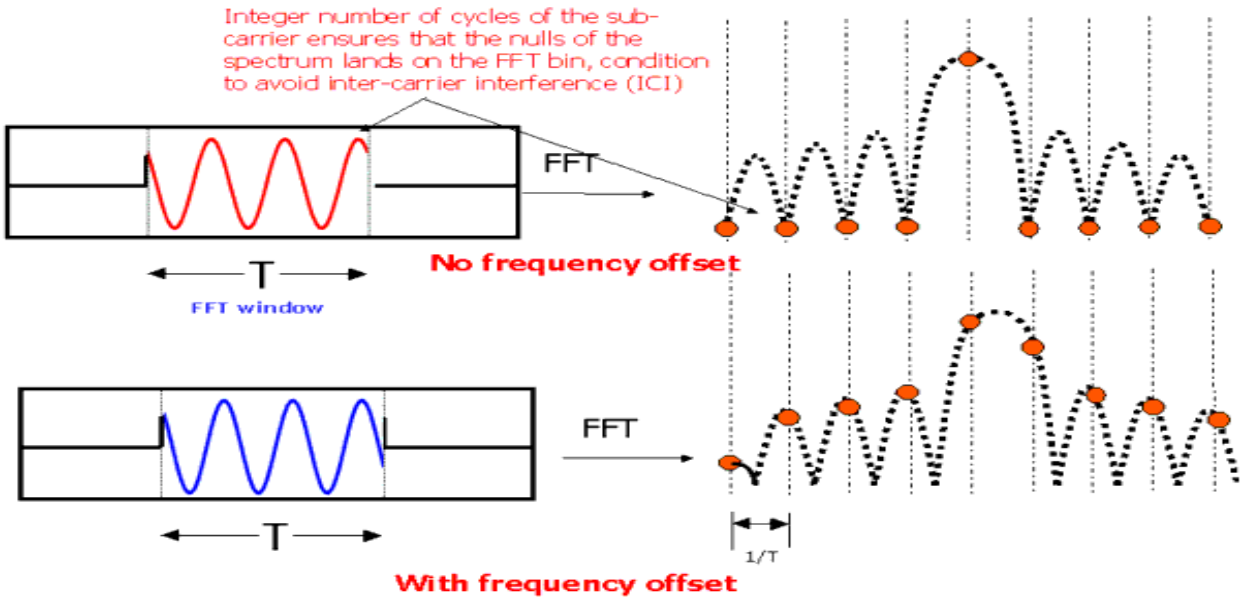

Fig 2.3: An OFDM Symbol with/without Channel Frequency Offset

The orthogonality of these subcarriers is proved mathematically by the famous principle of orthogonality:

$$\int_{m}^{n} F_a(t)F_b^*(t)dt = \begin{cases} K & fora = b \\ 0 & fora \neq b \end{cases} \qquad (2.1)$$

In the above equation * represents complex conjugate and the integral limits shows the symbol period i.e. [m,n] while $F_a(t)$ and $F_b(t)$represents a^{th} and b^{th} subcarriers respectively. The above equation dictates that in order for two sinusoids to be orthogonal, the integral of the product of the two sinusoids should be zero over a time period. And this can happen only when the frequency of the sinusoids will be integral multiple of each other.

The orthogonality principle requires that the subcarrier spacing should be $\Delta f = k/T_s$ (2.2)

Where T_s represents the symbol duration and k is normally taken as 1. So for N number of subcarriers the total passband bandwidth will be

$$B \approx N.\ \Delta f\ (Hz) \qquad (2.3)$$

2.4 Basic OFDM Model with mathematical description

The block diagram of OFDM is shown in the Fig. 2.4. Some optional blocks e.g. Channel Coding and Pilot insertion are not shown for

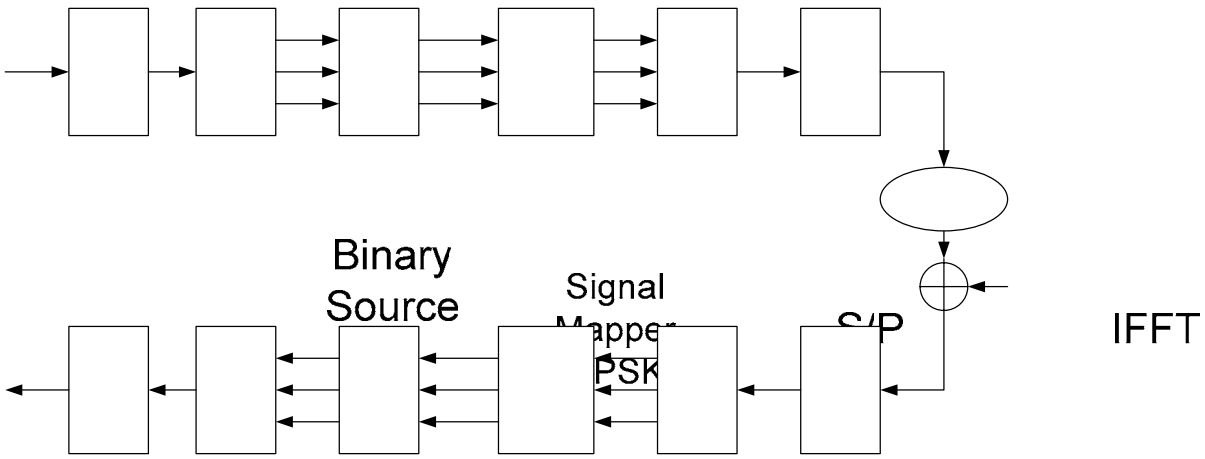

Fig 2.4. Block Diagram of OFDM System

simplicity purposes. These blocks will be incorporated and explained in the subsequent chapters.

In the simplest case, a binary data stream is fed to the Signal mapper block which introduces modulation mapping(e.g. BPSK, QPSK, QAM) into the signal. We have produced our results with BPSK, QPSK, 16-QAM and 64-QAM, and have made a comparison between all. After signal mapping the mapped symbol with N subcarriers is given by

$X_p=[X_p(0), X_p(1), X_p(2)....., X_p(N-1)]^T$ (2.4)

Then the signal is converted from serial to parallel format according to the size of the N-pt IFFT used. In our work we have used 512 point FFT otherwise specified. The parallel converted data is then passed through IFFT block. For the signal x(n) and subcarrier n (n=0,1,2 .....N-1), N-point IFFT produces the OFDM modulated symbol at time instant p as

$$X_p(k) = \frac{1}{N}\sum_{n=0}^{N-1} x(n) e^{-\frac{2\Pi j}{N}} \qquad (2.5)$$

Where $X_p(k)$ is given by

$X_p(k)=[X_p(0), X_p(1), X_p(2)....., X_p(\text{N-1})]^{\text{T}}$ (2.6)

IFFT block modulates the input mapped signal onto the subcarriers by multiplying it with a complex exponential. This step is called OFDM modulation. At the receiver end, the subcarriers are demodulated by an FFT, which performs reverse operation of an IFFT.

After taking IFFT, Guard interval is added in between two symbols i.e. we start the transmit block $\tilde{X}p$ with the last L symbols of $X_p(k)$.

$$\tilde{Xp} = \begin{cases} Xp + (N-L) & p = 0,1,2,3,.....L-1 \\ Xp - L & p = L, L+1,.....L+N-1 \end{cases} \qquad (2.7)$$

Guard interval prevents the aliasing of the symbols due to the multipath delay spread. The length of the guard interval G must be greater than the maximum channel delay spread D i.e. $D \leq G$

The signal is then passed through the passband modulation RF stage and is converted into the analog format to be put on to the channel which otherwise introduces severe impairments into the signal.

Assuming the channel consists of L discrete paths, the received signal at the receiver is given by:

$$y(n) = \sum_{l=0}^{L-1} h(n,l)x(n-l) + w(n) \tag{2.8}$$

Where *h(n,l)* represents the channel impulse response at instant *n* and *w(n)* represents the AWGN noise added at the receiver.

At the receiving end, after the removal of guard interval, the signal is passed through the FFT block which converts back the signal into frequency domain. The demodulated signal obtained after taking the FFT of the received signal is given by:

$$Y(m) = \sum_{k=0}^{N-1} \sum_{l=0}^{L-1} X_K H_l^{(m-k)} e^{-j2\Pi lk/N} + W_m \tag{2.9}$$

Where W_m represents the FFT of $w(n)$ and $H_l^{(m-k)}$ represents the FFT of the multipath fading channel impulse response i.e.

$$H_l^{(m-k)} = 1/N \sum_{n=0}^{N-1} h_{n,l} e^{-j\Pi n(m-k)/N} \tag{2.10}$$

After this the signal is reconverted to serial format and is then passed through the demapper block to get back the originally transmitted bit stream.

2.5 Inter-Block interference and its remedy

The OFDM symbols while passing through the channel gets elongated due to the delay spread of the channel. As far as the Delay Spread is less than or equal to the Time Period of the Symbol, there is no IBI occurring into the system. Delay spread refers to the maximum time lapse between the arrival of the first and the last multipath component. Multipath refers to the condition where the transmitted signal experiences reflections, diffractions and scattering which causes multiple echoes of the same signal to arrive at the receiver at the same time or delayed. This results in the leakage of one OFDM symbol energy in its adjacent symbols and generate a tail of energy that lasts much longer than expected as shown in figure 2.5 and 2.6[13].

In figure 2.5, the transmitted signal for the sequence 101101 shows a shape that is confined within its time period but this geometry in figure 2.6 after being received at the receiver is spilling its energy into the adjacent symbols causing an interference amongst the symbols resulting in the phenomenon called as Inter-Block Interference(IBI) or Inter-

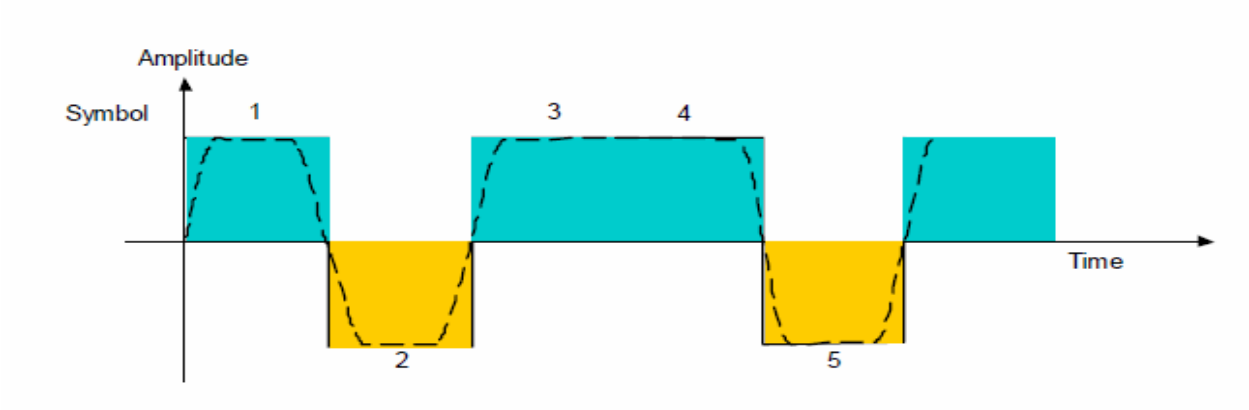

Fig 2.5: Sequence 101101 that is to be sent. The dashed line shows actual transmitted shape

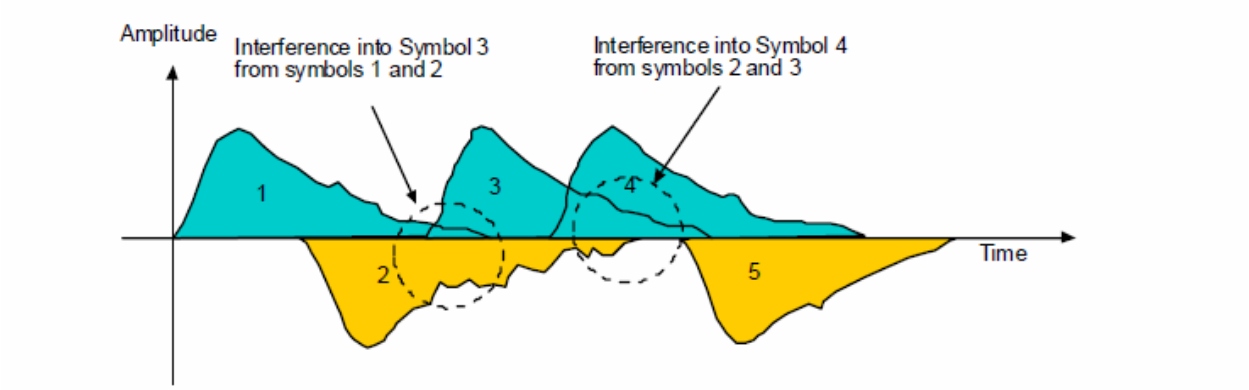

Fig 2.6: Received sequence of the transmitted shown in figure 2.5

Symbol Interference (ISI). Symbol here refers to the OFDM symbol and not the QPSK or QAM symbol.

IBI causes severe degradation of the signal quality. In order to cater-for the unwanted effects of ISI, method called Cyclic Prefix(CP) insertion is used. Other than Cyclic prefix insertion technique, ISI can be removed by using proper pulse shaping using Root-Raised Cosine

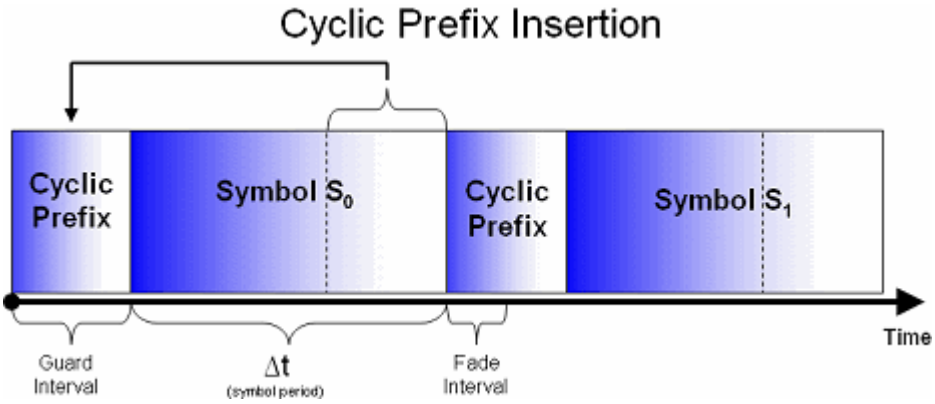

Fig 2.7: Cyclic Prefix addition in OFDM symbol

filtering approach in the systems where increased computational complexity doesn't matter. Our emphasis in this thesis would be on Cyclic prefix insertion method.

In Cyclic Prefix addition process, a 12%-25% portion from the end of the symbol is copied at the start. This causes the symbol to be elongated in the time-domain at the expense of extra bandwidth usage. So if multiple echoes of the same symbol are arrived at the receiver, the aliasing portion of the symbols would be the one that is replicated by coping the 1/4-1/8 fraction portion from the end to the start of the symbol. Thus only the duplicate subcarrier will get lost and the system would be saved from the adverse effects of Inter-Symbol Interference. Figure 2.7 shows CP introduction in the OFDM symbol.

2.6 Inter-Carrier interference (ICI) and its remedy

OFDM symbol consists of a number of subcarriers on which data is modulated. As discussed in Sec. 2.3, these subcarriers are essentially orthogonal to eachother. This is the reason that OFDM is a spectrally efficient technique due to overlapping of subcarriers in frequency-domain as shown in figure. 2.2. This overlapping requires the subcarriers to be perfectly orthogonal. The frequencies chosen for the subcarriers are such that the peak of one subcarrier matches the null of the other subcarriers. During the course of transmission due to a possible relative motion between the transmitter and receiver Doppler frequency is generated which is given by

$$y_d = \frac{v}{\lambda} 2\pi \cos(\theta) \qquad (2.11)$$

Here θ is the angle between velocity and communication link and is generally modeled as uniformly distributed between 0 to 2π, v is the receiver velocity and λ is the carrier wavelength.

Doppler frequency produces Channel Frequency Offsets (CFO) amongst the subcarriers(figure 2.3). These frequency offsets cause mismatch of the peaks and nulls of the subcarriers causing power leakage amongst different subcarriers of the same OFDM symbol resulting in a degradation of

the system performance [14]. This phenomenon is referred to as Inter-Carrier Interference (ICI). ICI is possible even if there is only one user in the system because it occurs due to the interference amongst the subcarriers of the same OFDM symbol.

Second cause of ICI is due to the synchronization issues between OFDM transmitter and receiver. The OFDM receiver oscillators for synchronization are unstable and produce frequency offset. This offset is negligible in the traditional communication system, but it causes severe degradations in OFDM system which is based on the Orthogonality of subcarriers. In most of the situations the oscillator frequency offsets varies from 20 ppm(parts per million) to 100 ppm [15].

Different approaches can be adopted for cancellation of the effects of ICI. These approaches include channel frequency offset estimation, windowing approach, polynomial cancellation coded (PCC) etc. In CFO estimation approach we send a pilot symbol prior to the OFDM symbol and based on the knowledge of the pilot symbol we estimate the Channel matrix whose inverse is then multiplied with the received OFDM symbol to equalize the induced CFO from the subcarriers.

The second approach supports the windowing method in either time or frequency domain, e.g. Nyquist windowing and Hanning windowing. The

third method is termed as ICI self-cancellation or Polynomial cancellation coded (PCC), where the repeated bits are transmitted to mitigate inter-carrier interference at the expense of bandwidth usage. In this thesis our emphasis will be on the first approach due to its effectivity, low computational complexity and better results. This method is explained in detail in chapter-4.

2.7 Advantages and disadvantages of OFDM

Like other techniques, OFDM has its own advantages and disadvantages. Some of the worth mentioning are given below.

2.7.1 Advantages Of OFDM

(i) Spectrally efficient technique because of overlapping of subcarriers

(ii) High data rate possible due to spectral efficiency

(iii) Robust to multipaths because of application of Cyclic Prefix

(iv) More resistant to frequency-selective fading due to division of channel into narrowband flat fading subchannels

(v) High performance gain possible by the integration of Turbo Codes

(vi) Computationally efficient because of the use of FFT/IFFT pair for modulation and demodulation

(vii) Offers superior shelter against co-channel interference and impulsive parasitic noise.

2.7.2 Disadvantages Of OFDM

(i) More sensitive to carrier frequency offsets than Single-carrier systems because of overlapped subcarriers. It requires proper channel equalization techniques at the expense of additional computational complexity at the receiver side.

(ii) High Peak-to-average Power ratio problem. It emerges because of the peaks of the signal amplitude at the transceivers getting out of the Active Region of the amplifiers. The existing result which is leaving some of the subcarriers unmodulated so as to keep the peaks within the Active Region limits, wastes the useful bandwidth.

2.8 Conclusion

In this chapter the salient features of OFDM technique have been discussed. These features depict that OFDM is a bandwidth efficient technique due to

division of a large bandwidth into narrowband overlapping and orthogonal subcarriers on which data is modulated. This makes OFDM a promising technique for the emerging wireless technologies e.g. 802.16e (WiMax), 802.11n(Wi-Fi), 802.11a/g(WLAN). Due to sensitivity of subcarriers of the channel frequency offsets produced due to a number of reasons including Doppler's shift, Tx-Rx mismatching etc, equalization technique is necessary to be implemented into OFDM. Alongwith this, proper error correcting codes further improves the system performance. These techniques will be the essence of the rest of the thesis.

Chapter-3

TURBO CODES

3.1 Background

The history of channel coding or Forward Error Correction (FEC) coding dates back to Shannon's pioneering work [16] in 1948, predicting that arbitrarily reliable communication is achievable with the aid of channel coding, upon adding redundant information to the transmitted messages.

The famous channel capacity equation formulated by Claud.A.Shanon for a band-limited channel with additive white Gaussian Noise is given by

$$C = B\log_2(1 + SNR) \tag{3.1}$$

where C is in bits/sec. Inspite of giving this formula, Shannon refrained from proposing explicit channel coding schemes for practical implementations.

Furthermore, although the amount of redundancy added increases as the associated information delay increases, he did not specify the maximum delay that may have to be tolerated, in order to communicate near the Shannonian limits [17].

The first Forward Error Correcting (FEC) codes were Hamming codes developed in 1950[18] capable of correcting single bit errors. Invention of

Convolutional FEC codes goes back to 1955 [19], which were discovered by Elias, Wozencraft and Reiffen [20,21], while Fano [22] and Massey [23], proposed there own algorithms for decoding. A major breakthrough in the history of convolutional error correction coding was the development of a maximum likelihood (ML) sequence estimation algorithm by Viterbi [24] in 1967. An interpretation of the Viterbi Algorithm (VA) was given by Forney's often-quoted work [25]. One of the first practical applications of convolutional codes was proposed by Heller and Jacobs [26] during the 1970s. All the above quoted work was focused on achieving the channel capacity benchmark set by Shannon in 1948.

The turbo codes principle was introduced in 1993 by C. Berrou, Glavieux and Thitimajashima [27] in Geneva congress where for the first time an error correcting code working within the range of 0.5 dB of the Shannon capacity limit was introduced. From the day of there introduction, Turbo codes have gained a lot of acceptance and these codes have been used with various communication techniques for error correction purposes. In our work we have integrated these codes in OFDM and have proved that the performance of the system has been improved tremendously.

3.2 Anatomy of Turbo Encoder

Broadly speaking, there are two types of Encoders in a communication system

(i) *Source Encoder:* It converts the input information sequence into a sequence of binary digits with minimum redundancy. Example is Huffman Coding.

(ii) *Channel Encoder:* It adds redundancy to the source encoded information sequence bits to minimize transmission errors. Example is Convolution Encoder, Turbo Encoder.

Our discussion in this chapter will be focused on the Turbo Channel Encoders. Since there introduction in 1993, several schemes of Turbo Codes have been proposed but the basic theme of all was the same i.e. "parallel concatenation of two or more Recursive Systematic Convolutional (RSC) encoders, all separated by an interleaver". A rate 1/3 Turbo Code Encoder is shown in figure 3.1.

The generator matrix of rate ½ component RSC encoder is given as

$$G(D) = \begin{bmatrix} 1 & \dfrac{g_1(D)}{g_0(D)} \end{bmatrix} \qquad (3.2)$$

here $g_0(D)$ and $g_1(D)$ are feedback and feedforward polynomial of degree v. In the encoder the same information sequence is encoded twice but in

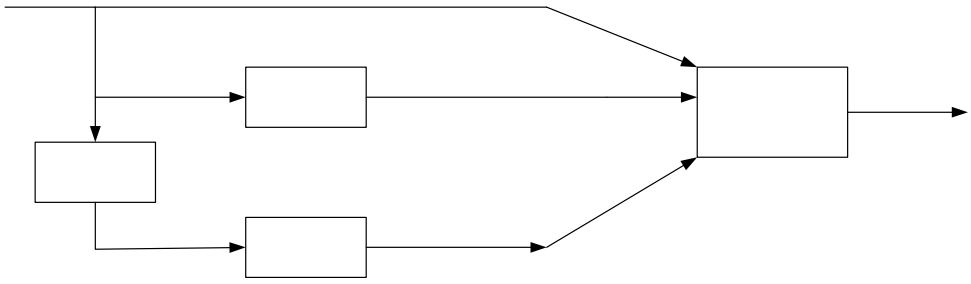

Figure 3.1: General diagram of a Turbo code encoder

an interleaved fashion, the reason of which is given in the section 3.2.1. The first component RSC encoder of rate 1/2 works directly on the input bit stream, it has two outputs, systematic and parity bit 1. In the second encoder the interleaved version of the same information sequence is fed. But only the parity sequence is transmitted for RSC convolutional encoder-2. The information sequence and the parity check sequences are multiplexed and punctured to generate the turbo code sequence of rate 1/3.

The task of the interleaver is to scramble the bits in a predetermined random fashion that is to be recovered at the receiver side. The choice of interleaver plays an important role in the overall system performance and will be discussed in detail in section 3.4.

3.2.1 Why Parallel Concatenation

The parallel concatenation of the RSC Encoders is important for two reasons. The first reason is the tendency of producing high weight output codes because of efficient decoding of bit 1. So if the input to the second encoder is interleaved, the output produced by the second encoder is less correlated from the output of the first encoder. So if the output produced by one of the encoder is low weight then there are very less chances that the output produced by the second encoder will also be of less weight. So the chances of production of a low weight output code word are very less.

Second reason is the employment of divide-and-conquer strategy for decoding. If the input to the second decoder is scrambled, its output will be uncorrelated from the output of the first encoder. Thus the corresponding two decoders will gain more from information exchange.

3.2.2 Recursive Systematic Convolutional (RSC) Encoder:

The component encoder used in our simulation for Turbo Encoder is RSC Encoder. The structure of the RSC encoder is derived from a non-recursive Convolutional encoder by feeding back one of its parity bit output to the

input[24]. Figure 3.2 shows the structure of a non-recursive convolution encoder of rate ½.

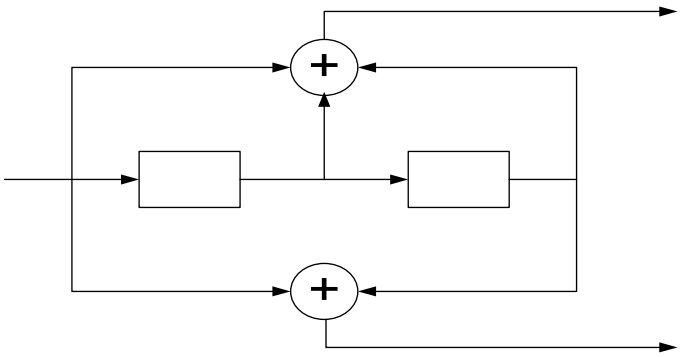

Figure 3.2: A non-recursive Convolutional Encoder with rate ½

This convolutional encoder is represented by the generator sequence g_1=[1 1 1] and g_2=[1 0 1]. The corresponding Generator matrix is represented as G=[g_1 g_2]. A generator matrix is a basis for a linear code which generates all the possible code words for a given [n,k] code.

Input sequence D

For the corresponding RSC convolutional encoder, the generator matrix is represented as G=[1, g_1/g_2] where the first output represented by g_1 is fed back to the input. In the above representation, 1 denotes the systematic output, g_2 represents the feed-forward output g_1 is the input to the RSC encoder. It is called systematic code because the input sequence is exactly been replicated in the output as well. Figure 3.3 depicts the resulting RSC encoder.

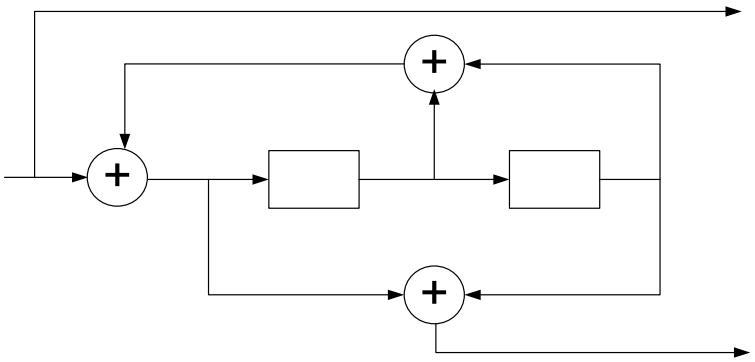

Figure 3.3: An RSC Convolutional Encoder with rate ½

In our simulation, the arrangement that we have used is to transmit all the systematic bits from the first RSC encoder and then one parity bit from each of the two component RSC encoder of rate ½, so the overall code rate comes out to be 1/3. The generator sequences used were [1 1 1 1] and [1 1 0 1] and have been borrowed from the work of Benedetto[39]. Output sequence from the encoder is

$S_1 P_1^1 P_1^2 \; S_2 P_2^1 P_2^2 \; S_3 P_3^1 P_3^2 \; S_4 P_4^1 P_4^2 \; S_5 P_5^1 P_5^2$ ---

where the subscript represents bit number and the superscript represents the component RSC Convolutional Encoder number.

3.3 Turbo Decoding

A basic structure of a Turbo decoder consists of two component decoders that exchange soft information amongst eachother to improve the final

estimate about the decoded bits. Each of this component decoder is based on one of the two basic Turbo decoding algorithms namely

i. Maximum A Posteriori (MAP) Algorithm

ii. Soft Output Viterbi Algorithm (SOVA)

We have used MAP decoding algorithm in our work and this ll be explained with due details in the following lines. SOVA will be briefly explained to complete the discussion.

3.3.1. Maximum A Posteriori (MAP) algorithm

The iterative turbo decoding consists of two component decoders serially concatenated via an interleaver, identical to the one in the encoder as shown in figure 3.4.

The first MAP decoder takes as input the received systematic information sequence C^s and the received parity sequence generated by the first encoder $C^{1,p}$. The decoder then produces a soft output in the form of Log-Likelihood ratio (LLR) which is interleaved and used to produce an improved estimate of the a-priori probabilities of the information sequence for the second decoder. The LLR produced by Deocder-1 is given by

$$LLR(d) = \ln\left(\frac{P(d=1)}{P(d=0)}\right) \qquad (3.3)$$

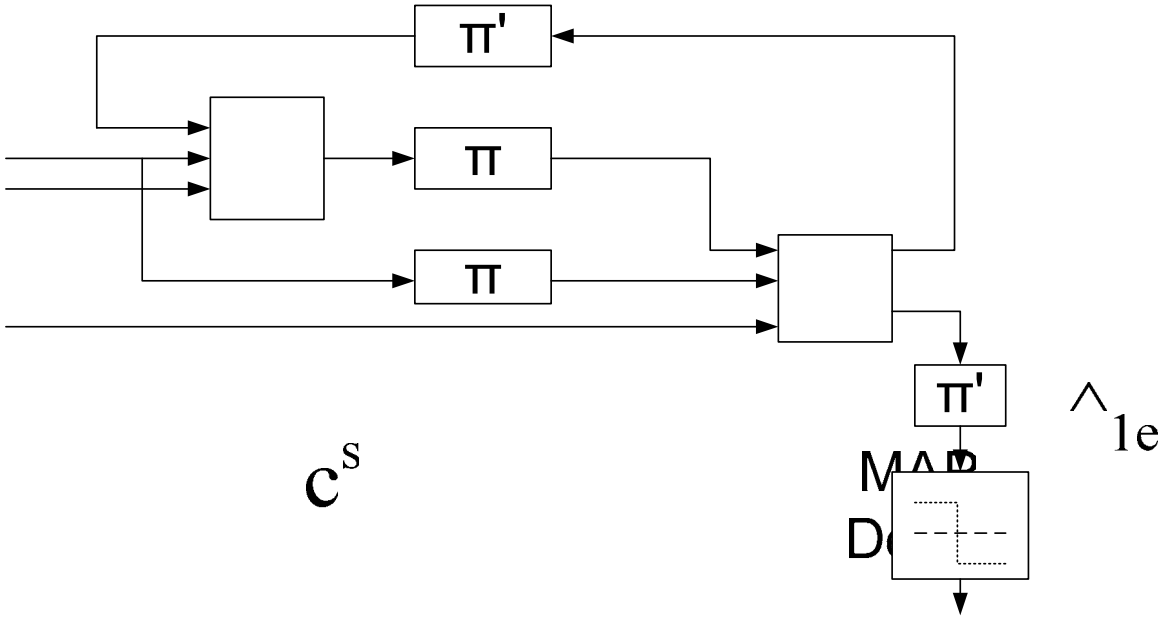

Figure 3.4: A Turbo Decoder based on two component MAP Decoders

The third input to the first decoder is the a-priori probability of the second decoder which was taken as 0.5 in the first iteration.

For the MAP decoder-2, the two inputs are the interleaved received sequence $\overset{\upsilon}{C}^{S}$ and the received parity sequence produced by the second encoder $C^{2,p}$. The second MAP decoder produces its own soft output which is used to improve a priori probability of the information sequence at the input of the first MAP decoder. Thus the final estimate of the decoder keeps on improving relative to a single operation serially concatenated encoder. The extrinsic information produced by the two decoders diverges from the mean 0.5 as the iterations carry on and after n number of iterations a hard decision is taken at the output of MAP decoder # 2. A +ive value of the

output of the MAP decoder depicts a received 1 and a –ive value represents a 0 bit .

Now the LLR produced by the first MAP decoder for rate 1/n component code is given mathematically as

$$\Lambda_1(C_t) = \log \frac{\sum_{l',l=0}^{M_s-1} \alpha_{t-1}(l') p_t^1(1) \exp(-\frac{\sum_{j=0}^{n-1}(r_{t,j} - x_{t,j}^1(l))^2}{2\sigma^2}) \beta_t(l)}{\sum_{l',l=0}^{M_s-1} \alpha_{t-1}(l') p_t^1(0) \exp(-\frac{\sum_{j=0}^{n-1}(r_{t,j} - x_{t,j}^0(l))^2}{2\sigma^2}) \beta_t(l)} \quad (3.4)$$

where $p_t^1(o)$ and $p_t^1(1)$ are the a priori probability at the input of MAP dec-1 taken as 0.5 each in the first iteration. $p_t^2(o)$ and $p_t^2(1)$ are the a priori probability at the input of the MAP dec-2.

The terms ,α,β,γ are written as

$$\alpha_t(l) = P_r\{S_t = l, \mathbf{r}_1^t\}$$

$$= \sum_{l'=0}^{M_s-1} P_r\{S_{t-1} = l', S_t = l, \mathbf{r}_1^t\}$$

after certain mathematical manipulations, it can be written as

$$= \sum_{l'=0}^{M_s-1} \alpha_{t-1}(l') . \sum_{i\in(0,1)} \gamma_t^i(l', l) \quad (3.5)$$

for t=1,2,3,4,…….τ

for t=0 we have the boundary conditions $\alpha_o(0)=1$ and $\alpha_o(l)=0$ for $l\neq 0$

Similarly, $\beta_t(l)$ can be written as $\beta_t(l) = P_r\{\mathbf{r}_{t-1}^{\tau} \mid S_t = l\}$

$$= \sum_{l'=0}^{M_s-1} P_r\{S_{t+1} = l', \mathbf{r}_{t+1}^{\tau} \mid S_t = l\}$$

after certain mathematical manipulations it can be written as

$$= \sum_{l'=0}^{M_s-1} \beta_{t+1}(l') \sum_{i\in(0,1)} \gamma_{t+1}^{i}(l,l') \qquad (3.6)$$

for $t=\tau-1, \ldots\ldots\ldots\ldots..2,1,0.$

The boundary conditions are $\beta_\tau(0)=1$ and $\beta_\tau(l)=0$ for $l \neq 0$

And γ can be written as

$$\gamma_t^i(l',l) = P_r\{C_t = i, S_t = l\}, \mathbf{r}_t \mid S_{t-1} = l'$$

$$= \frac{P_r\{\mathbf{r}_t, c_t = i, S_t = l, S_{t-1} = l'\}}{P_r\{S_{t-1} = l'\}}$$

and after mathematical manipulations it can be written in the final form as

$$= \begin{Bmatrix} p_t(i)\exp\left(-\dfrac{\sum_{j=0}^{n-1}(r_{1,j}^i - x_{t,j}^i(l))^2}{2\sigma^2}\right) for (l,l') \in B_t^i \\ 0 otherwise \end{Bmatrix} \qquad (3.7)$$

Now we get rewriting equation 3.5

$$\Lambda_1(c_t) = \log \frac{p_t^1(1)}{p_t^1(0)} + \log \frac{\sum_{l',l=0}^{M_s-1} \alpha_{t-1}(l') \exp\left(-\frac{(r_{t,0} - x_{t,0}^1)^2 \sum_{j=0}^{n-1} (r_{t,j} - x_{t,j}^1(l))^2}{2\sigma^2}\right) \beta_t(l)}{\sum_{l',l=0}^{M_s-1} \alpha_{t-1}(l') \exp\left(-\frac{(r_{t,0} - x_{t,0}^0)^2 \sum_{j=0}^{n-1} (r_{t,j} - x_{t,j}^0(l))^2}{2\sigma^2}\right) \beta_t(l)} \tag{3.8}$$

Since the code is systematic so $x_{t,0}^1 = 1$ and $x_{t,0}^0 = -1$. Thus $\Lambda_1(C_t)$ could be further decomposed into

$$\Lambda_1(c_t) = \log \frac{p_t^1(1)}{p_t^1(0)} + \frac{2}{\sigma^2} r_{t,0} + \Lambda_{1e}(c_t) \tag{3.9}$$

where $$\Lambda_{1e}(c_t) = \log \frac{\sum_{l',l=0}^{M_s-1} \alpha_{t-1}(l') \exp\left(-\frac{\sum_{j=0}^{n-1} (r_{t,j} - x_{t,j}^1(l))^2}{2\sigma^2}\right) \beta_t(l)}{\sum_{l',l=0}^{M_s-1} \alpha_{t-1}(l') \exp\left(-\frac{\sum_{j=0}^{n-1} (r_{t,j} - x_{t,j}^1(l))^2}{2\sigma^2}\right) \beta_t(l)} \tag{3.10}$$

Here $\Lambda_{1e}(C_t)$ is called extrinsic information and this extrinsic information when interleaved and fed to the 2nd MAP decoder becomes its a priori information. Similarly the 2nd MAP decoder calculates its extrinsic information, the deinterleaved version of which acts as a priori information for MAP dec-1 improving its estimate. In this way the two decoders gain from eachother's information. In the final iteration, depending upon the sign of the LLR generated by MAP decoder-2, the bit is decoded as 1 or 0. A

+ive sign of the LLR represents the decoded bit to be a 1 and a –ive sign represents a decoded bit 0.

3.1.1.1: Computational Complexity:

The computational complexity of Turbo decoder is given by the following table[28]:

Operation	Maximum *a posteriori* Algorithm
Maximization	2M-1
Addition	4M
Multiplication	10M
Table Look Up	0
Total Operation	14M
Total # of Operations	30M-1

Figure 3.5: Table for total number of operations in a Turbo MAP decoder

M = Total states of decoder. For constraint length=3 the total number of states , M=8

Thus, total number of operations per bit = 30 x 8 – 1 =239 operations

BPSK:

The data rate of the proposed model (Figure 5.7) for BPSK modulation scheme is 11.57 Mbps.

Therefore the total number of operations for BPSK modulation scheme per second is given by

11.57 x 239 = 2.765 Gops

QPSK:

The data rate of the proposed model (Figure 5.7) for QPSK modulation scheme is 23.15 Mbps.

Therefore the total number of operations for BPSK modulation scheme per second is given by

23.15 x 239 = 5.536 Gops

16-QAM:

The data rate of the proposed model (Figure 5.7) for 16-QAM modulation scheme is 46.25 Mbps.

Therefore the total number of operations for BPSK modulation scheme per second is given by

46.25 x 239 = 11.053 Gops

64-QAM:

The data rate of the proposed model (Figure 5.7) for 64-QAM modulation scheme is 69.37 Mbps.

Therefore the total number of operations for BPSK modulation scheme per second is given by

69.37 x 239 = 16.579 Gops

3.3.2. Soft Output Viterbi Algorithm (SOVA)

The scope of our research is limited to MAP decoding algorithm, SOVA has been briefly explained here for completion of the discussion regarding turbo decoding algorithms. The Soft Output Viterbi Algorithm (SOVA) is an extension of the predecessor Viterbi Algorithm (VA). But its increased computational complexity and degraded performance makes MAP algorithm a first choice for the researchers. The Viterbi algorithm finds the most likely path through trellis diagram given the received signal bits. The conditional probability is given by the Baye's Rule as:

$$P(x/y) = \frac{P(y/x)P(x)}{P(y)} \qquad (3.11)$$

in the above equation, $P(x)$ and $P(y)$ represents the a-priori probability of transmitted and received symbol respectively. Assuming that the a-priori probabilities of the bits are statistically independent, and $P(x)$ is replaced by $P(u)$ which is the a priori probability of sign vector u then equation (3.11) can be written as

$$P(x/y) = \frac{1}{P(y)} \prod_{i=1}^{N} p(y_i/x_i) \prod_{k=1}^{K} p(u_k) \qquad (3.12)$$

For the antipodal binary signaling, $x_i \in \{\pm 1\}$, we term the a priori LLR vectors as:

$$L_i^c = \log \frac{p(y_i / x_i = +1)}{p(y_i / x_i = -1)} \quad ; \quad L_k^c = \log \frac{p(u_k = +1)}{p(u_k = -1)} \quad (3.13)$$

The channel LLR can also be written as

$$L^c = \frac{2}{\sigma^2} A_y \quad (3.14)$$

Thus the conditional probability of any sequence that has been transmitted is given by

$$P(x / y) = C \exp(\frac{1}{\sigma^2} u(x)) \quad (3.15)$$

Here C is a constant and *u(x)* is a criterion defined by

$$u(x) = \frac{\sigma^2}{2}(x.L^c + u.L^a) \quad (3.16)$$

if we have only two possible antipodal results of an event, x and $\hat{x}$.

Then $$P(\hat{x}/ y) = 1 - P(x/ y) \quad (3.17)$$

and thus the LLR is given by

$$L(\hat{x}) = \log \frac{P(\hat{x}/ y)}{P(x/ y)} = \frac{1}{\sigma^2}(u(\hat{x}) - u(x)) \quad (3.18)$$

This is the value of LLR that is exchanged as soft information between the SOVA Decoders to improve the final estimate.

3.4 Interleaving

As discussed in section 3.2, interleavers play crucial role in the performance of turbo codes. The basic role of the interleaver is to scramble the bits in a random albeit predetermined order to avoid burst error by spreading the burst of errors into a number of symbols.

A number of Interleavers are available each giving different permutations. We have simulated our results using the high performing Random Interleaver and have compared the performance of different modulation schemes in Rayleigh as well as AWGN channels and different number of iterations of turbo decoder. Now we will briefly explain the functionality of a few commonly used interleavers.

3.4.1 Row-Column Interleaver

Simplest of all the interleavers and included in the block-type interleavers, in a row-column interleaver the data is written row-wise and is read column-wise. See figure 3.5(b). Due to its simplest operation it provides very less randomness.

Input				
x1	x2	x3	x4	x5
x6	x7	x8	x9	x10
x11	x12	x13	x14	x15

Figure 3.6(a): Input to the Interleaver

Row-Column Interleaver														
x1	x6	x11	x2	x7	x12	x3	x8	x13	x4	x9	x14	x5	x10	x15

Figure 3.6(b): Output of Row-Column Interleaver

Helical Interleaver Output														
x11	x7	x3	x14	x10	x1	x12	x8	x4	x15	x6	x2	x13	x9	x5

Figure 3.6(c): Output of Helical Interleaver

3.4.2 Helical Interleaver

Here the data is written row-wise and is read diagonally. Again the small amount of scrambling doesn't show much improved performance. See fig. 3.5(c).

3.4.3 "Odd-Even" Interleaver

This type of encoder does the interleaving as a three step process. For the rate ½ Systematic Convolutional Encoder, the one that we used as component encoder for our rate 1/3 encoder, first of all the odd positioned bits are taken as it is and are mapped on the corresponding positions in the output memory.

x1	x2	x3	x4	x5	x6	x7	x8	x9	x10	x11	x12	x13	x14	x15
y1		y3		y5		y7		y9		y11		y13		y15

Figure 3.7(a): Encoder odd-positioned output (without interleaving)

Then the output of the interleaver is interleaved with a row-column interleaver (Fig.3.5(b)) and the even-positioned coded bits are stored as follows.

x1	x6	x11	x2	x7	x12	x3	x8	x13	x4	x9	x14	x5	x10	x15
	Z6		z2		z12		z8		z4		z14		z10	

Figure 3.7(b): Encoder even-positioned output (with row-column interleaving)

In the third step both these outputs i.e. given in 3.6(a&b) are multiplexed to find the final output.

Y1	Z6	Y3	z2	Y5	z12	Y7	z8	Y9	z4	Y11	z14	Y13	z10	Y15

Figure 3.7(c): Final output of the Encoder

3.4.4 “Random” Interleaver

The Random Interleaver rearranges the elements of its input vector using a random permutation. The Random or Pseudo-Random Interleavers are defined by a pseudo-random number generator or a lookup table where all the integers from 1 to N can be generated. The efficient or inefficient scrambling of data depends upon the size of the interleaver generated and the amount of data that is scrambled. Being one of the best performing interleavers, the least computational complexity makes it a good choice for implementation. Random interleaver requires a memory for memorizing the interleaving pattern so as to reproduce it at the deinterleaving side.

3.4.5 High Spread Deterministic Interleaver

Introduced in 2005, High Spread Deterministic Interleaver [29] combines both the qualities of regular permutation of interleaver and decorrelation property of decoder. The Interleaver works on increasing minimum effective free distance d_{min} between the adjacent interleaved symbols. The systematic design and least memory requirement makes the interleaver best suited for parallelism which is a basic requirement of Turbo codes. The BER of the system can be lowered either by increasing the interleaver size or by increasing the d_{min}. Increasing the interleaver size may not be a desirable solution as it increases the queuing delay of the system to the unacceptable limits for some real time applications. So second option that is, increasing the d_{min} can prove to be a good solution.

The spread associated with two write indices i and j is can be written as

$$S(i,j) = |\pi(i) - \pi(j)| + |i - j| \tag{3.19}$$

$$S_{\min} = \min_{i,j} S(i,j) \tag{3.20}$$

Where $\pi(i)$ and $\pi(j)$ represents the interleaved positions of indices i and j respectively. $S_{\min}$ is the minimum value of $S(i,j)$ for all the possible permutations of i and j.

3.5 Conclusion

In this chapter we have discussed Turbo Codes with its major features. We have talked about the formation of a Turbo Encoder using RSC Encoders of different generator matrices. We have noticed the impact of generator matrix on the output code. Alongwith this, we have observed the MAP decoding algorithm with its mathematical details. Last portion of the chapter puts a light on different types of interleavers and discusses their advantages and disadvantages. This chapter shows that Turbo codes are best option for error correction in OFDM. When combined with a good equalization technique it can improve the overall system performance to a large extent.

CHANNEL ESTIMTION AND EQUALIZATION

4.1 Introduction

Channel estimation and equalization plays a key role in a communication system. Multipath propagation and Doppler spread have a strong negative impact on the bit error rate of any wireless transmission technique. The mobile radio channel impairments cause a signal at the receiver to distort or fade significantly. Severe performance loss is attained if the effect of these impairments is not equalized properly. This equalization requires the estimation of channel taps. A channel estimate is a mathematical estimate of the channel taps. Several schemes for channel estimation and equalization are discussed in this chapter. But all this jargon requires some prior knowledge of a wireless channel and its different characteristics. So in the start of the chapter we discuss the basics of a wireless channel and then after explaining the basic terminologies we'll move to the debate of channel estimation and equalization.

4.2 Wireless Channel and its Characteristics

A wireless channel refers to bandwidth allocated to a single connection, which may be fixed or varying in time. In fact a wireless channel is a sub spectrum of the allocated spectrum used to carry the data of a single user.

The characteristics of wireless channel plays a key role in the communication system, because these are the channel characteristics that dictate how intact data is received at the receiver. These characteristics play a central role in the selection of an appropriate equalizer for the system. The propagation characteristics include path loss, diffraction (shadowing), multipath effect, Doppler effect, fading etc. These terminologies are briefly explained below.

4.2.1 Path Loss

Path loss refers to the reduction in power density of an electromagnetic wave during its propagation through the medium. Path loss plays a vital role in the analysis and statistics of the telecommunication system. Path loss depends upon a number of parameters that include terrain contours, environment (urban or rural), propagation medium (moist or dry air), the propagation space between the transmitter and the receiver and the location and height of antennas. Path loss includes propagation losses caused by the natural expansion of the wave front in free space (that takes the shape of an increasing sphere).

Path loss is expressed in dB and is given by the formula

$$L_{pl}=10\ n \log_{10}(d) + L_{sys} \ (\textit{decibels}) \qquad (4.1)$$

In the above formula, n refers to the path loss exponent. d is in meters and represents the distance between transmitter and receiver and L_{sys} refers to the losses due to the system and includes the circuitry losses.

4.2.2 Diffraction

When the radio wave strikes an object with sharp edges, it is scattered in all directions. This redistribution of the intensity of radio waves in space is called Diffraction. Diffraction plays an important role in the propagation of radio signals through the curved surface of the earth. Secondary waves are generated from the diffracted waves and these are present throughout the space including behind the obstructing object and gives rise to a bending of waves causing propagation even behind the obstacles as shown in figure 4.1.

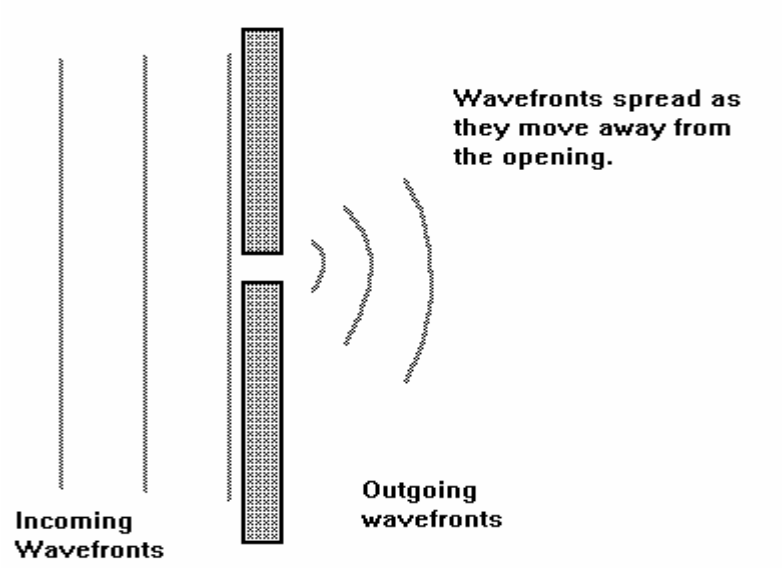

Figure 4.1: An incoming wave diffracted from a small opening

4.2.3 Doppler's effect

Whenever there is a relative motion between the transmitter and the receiver, the received frequency is not always the same as the transmitted frequency. When both are moving towards eachother the received frequency is higher than the transmitted one and if they are moving away from eachother, the received frequency is lower than the transmitted frequency. This phenomenon is referred to as Doppler effect. Doppler spread is the measure of the spectral broadening caused by the time rate of change of mobile radio channel. For a transmitted signal of frequency f_c, the received signal spectrum called the Doppler spectrum has the components in the range of fc – f_d to fc + f_d. Where f_d is the Doppler frequency and is a function of relative velocity between the transmitter and receiver. It is given by

$$f_d = \frac{v_r}{\lambda}\cos(\theta) \qquad (4.2)$$

Where f_d represents Doppler frequency, v_r is the relative velocity, λ is the carrier wavelength and θ is the angle between velocity and communication link and is generally modeled as uniformly distributed between 0 to 2π. As discussed in section 2.6, the Doppler spread is majorly responsible for the disturbance of the orthogonality of the subcarrier which causes inter-carrier interference amongst the subcarriers. The two most important fading effects

that are generated due to doppler's effect are Slow and Fast fading. Slow fading refers to the case when the Coherence time T_c of the channel is much greater than the symbol time, T_s. That is

$$T_c >> T_s$$

Similarly fast fading refers to the case when the channel impulse response changes at a rate much faster than the transmitted baseband signal. In this case

$$T_c << T_s$$

4.2.4 Mulipath Effect

Multipath is the propagation phenomenon in which multiple copies of the radio signal are received at the receiver with a small time delay via two or more than two different paths. It occurs due to the bouncing off the signal from different terrestrial objects such as mountains, buildings, planes etc. Each of received component has its own amplitude (because of unique path from any other multipath component) , phase and time delay. All these multipath components are added at the receiver constructively or destructively to give rise to a resultant signal of high or low amplitude.

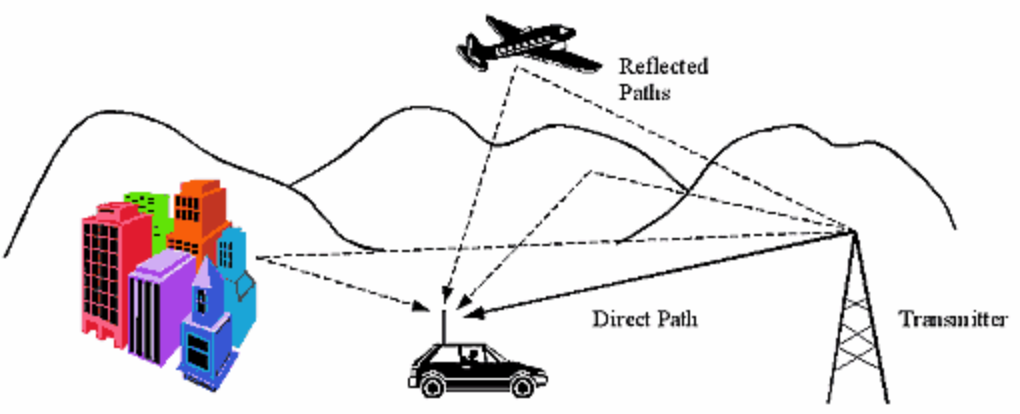

Figure 4.2: Multipath Propagation Phenomenon (Courtesy:Eric Lawery, "Suitability of OFDM as a modulation technique for wireless telecomm. With a comparison with CDMA", *BE dissertation*,James Cook University)

Alongwith this, each multipath component has a different Doppler frequency because the distance travelled by it 'ld be different from the other multipath components.

The two most significant effects of multipath propagation phenomenon include a rapid variation in the amplitude of the received signals which requires proper equalization at the receiving end and secondly the time dispersion in the received signal causes the adjacent symbol blocks to get elongated in time-domain which causes aliasing of the adjacent symbol blocks if are not proper cyclically prefixed.

Two multipath fading models have been standardized by keeping in view the rapid variation in the amplitude of the received signal. These two models are explained with brief details in the coming lines.

4.2.4.1 Rayleigh Multipath fading model

Rayleigh fading model is an appropriate model when there are too many objects in the communication environment and there doesn't exist any Line Of Sight (LOS) component in the system. All the multipath components that are received are the bounced off components having independent amplitude, phase and frequency components and don't have any LOS component. A Rayleigh fading channel is modeled in the complex baseband as

$$c(t) = \frac{1}{N}\sum_{i=1}^{N} A_I e^{j(2\Pi f_c t + \Phi_i)} \qquad (4.3)$$

Here A_i is the amplitude of the i^{th} complex sinusoid and φ_i is the random phase uniformly distributed from 0 to 2π, f_{ci} is the Doppler frequency. N is the total number of complex sinusoids making up the channel. Most of the practical environments obey Rayleigh distribution. We have also tested our proposed OFDM model on the Rayleigh channel with AWGN noise added.

A Rayleigh distribution function is actually an envelop of two quadrature Gaussian signals and is generated in MATLAB as:

Y=rand(n) + jrand(n) (4.4)

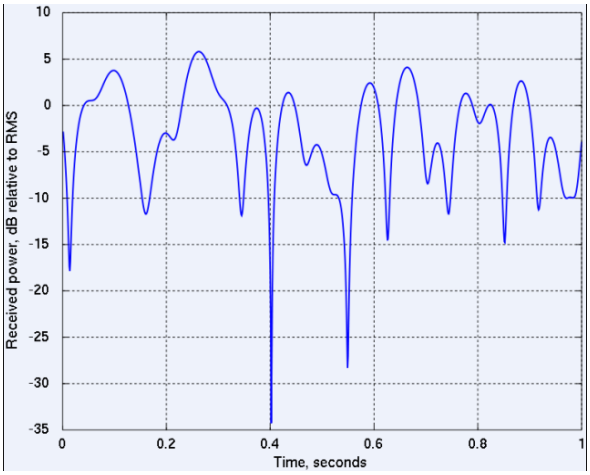

Figure 4.3: Rayleigh distributed fading

4.2.4.2 Rician Multipath fading model

Whenever the multipath environment has a strong dominant LOS component, the fading obeys Rician distribution. In the rician distribution the different multipath components arriving at the receiver with a time delay and different phases are superimposed on a strong dominant signal, which is the LOS component. The overall effect of this is like adding a dc component to the random multipath signal. But it should be remembered that if the dominant LOS gets weaker the Rician distribution began resembling a Rayleigh distribution.

As in most of the practical scenarios, the LOS component is absent due to the presence of a number of obstacles between transmitter and receiver. For the proposed simulated model, the distribution that is used is

Rayleigh distribution. Rician distribution is introduced here to complete the discussion.

4.3 Channel Estimation

As the transmitted signal travels over the channel, it is distorted because of the impairments introduced by the channel, discussed in section 4.2. Alongwith this, noise and interfering signals that originates from other sources, contaminate the output of the channel that results in the corrupted version of the transmitted signal. The function of the receiver is to operate on the received signal and to reverse the effects of the channel introduced impairments from it before doing any further operation on it. It has to reconstruct a recognizable form (i.e. produce an estimate) of the original message signal and deliver it to its destination [30].

This characterization of the effects of the physical medium on the input signal is termed as Channel Estimation process. And using these characterized effects of the channel to produce a recognizable form of the input sequence is called Equalization procedure.

4.4 Classification of Channel Estimation techniques for OFDM

Depending upon the requirements and fading environment, a number of channel estimation procedures can be adopted. The choice of channel

estimation strategy depends upon a number of parameters e.g. channel conditions, fading conditions, available bandwidth, computational complexity etc. But broadly speaking all these channel estimations and

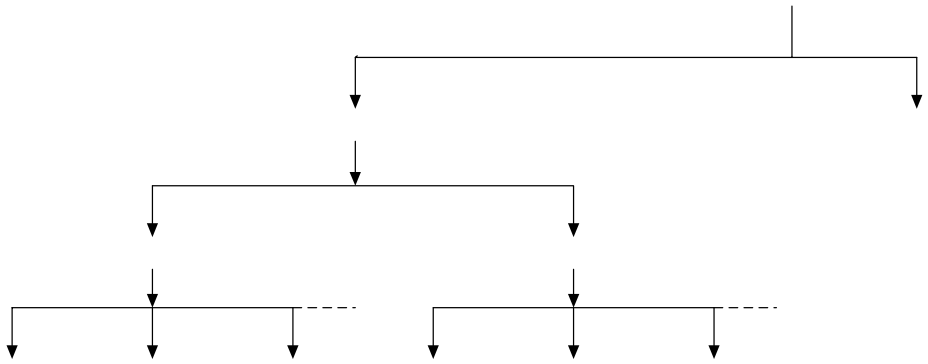

Figure 4.4: Classification of Channel Estimation Techniques

processes can be divided into two main classes; namely Pilot-assisted and non-pilot assisted. Figure 4.4 shows a pictorial view of the classification scheme of the different types of channel estimation strategies. Each of this strategy is explained briefly in the following lines.

Pilot Ass

4.4.1 Pilot assisted channel estimation

Comb Type

The most commonly used channel estimation technique is pilot-assisted channel estimation. Whenever the channel impulse response is varying and is unpredictable (as it is in most of the cases), we use pilot-assisted scheme. In this scheme the channel response is found out by sending pilot tones prior/parallel to the information signal. These pilot tones while their passage

LSE MMSE Zero Forcing

through the fading channel, accommodate the channel response. On the receiving end, the receiver which knows the originally transmitted pilot tones prior to the transmission, applies certain algorithm to find out the channel taps. Channel taps refer to the number of corresponding time samples of the channel impulse response. This process is called channel estimation. Based upon these channel taps, the receiver nullifies the channel response from the received information symbols to get the originally transmitted data information symbols. This process is called Equalization.

Pilot-assisted channel estimation is further divided into two types.

- Block-type Channel Estimation
- Comb-type Channel Estimation

The basic difference between the two types of channel estimation strategies is the way pilot tones are inserted into the information symbols.

4.4.1.1 Block-type Channel Estimation

In block-type channel estimation scheme, a few OFDM symbols are dedicated for the pilot tones. All the subcarriers in these OFDM symbols are dedicated for modulating pilot data and are used for estimation of the channel impulse response. Figure 4.5(a) shows a schematic view of the block-type pilot insertion technique.

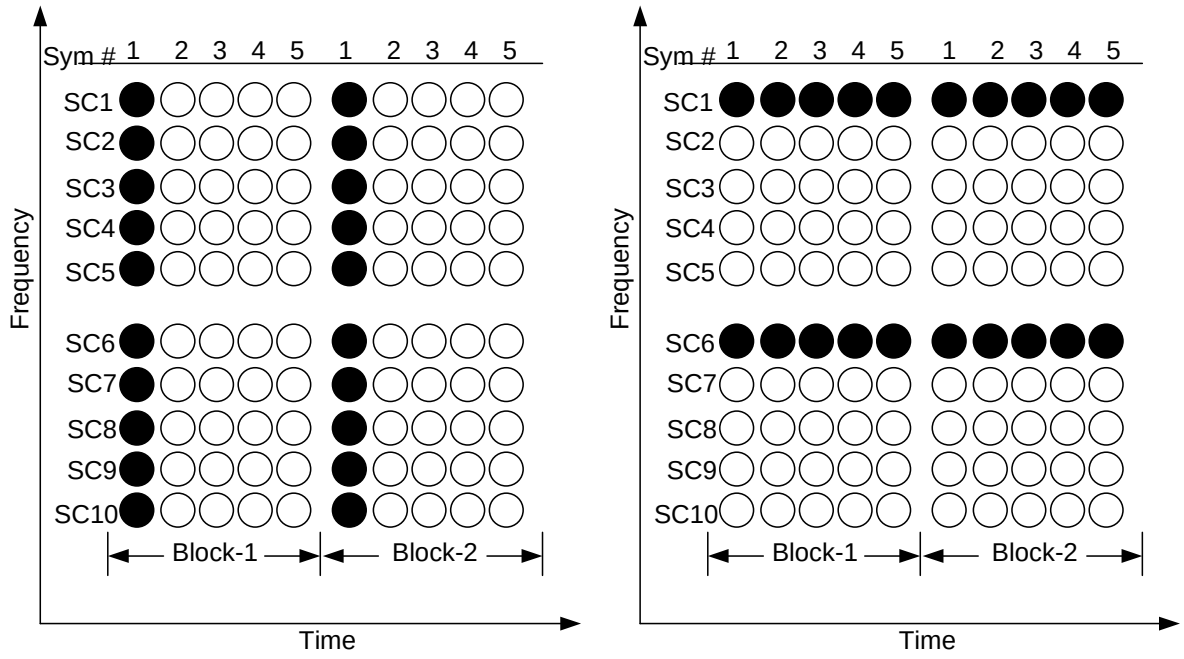

SC=Sub Carrier # , Sym=OFDM symbol # , ● =Pilot data, ○ = Information data

(a) Block-type pilot assisted CE (a) Comb-type pilot assisted CE

Figure 4.5: Schematic representation of Block-type and Comb-type pilot tone insertion technique

Figure 4.5(a) shows that for the case of Block-type channel estimation method, all the subcarrier of a few OFDM symbols carry pilot data. Based upon the channel impulse response achieved from the pilot OFDM symbols, the calculated channel taps are used for equalization of the upcoming data symbols till the arrival of the next Pilot symbol [31]. This method works very well for slow fading environment in which the channel impulse response remains almost the same within an OFDM block.

In order to achieve the channel taps a number of algorithms are used depending upon the trade-off between computational complexity and results, commonly used three of these methods are briefly explained below

(a) Zero Forcing algorithm

Proposed in 1965 by Lucky [32], one of the earliest and simplest equalizers, zero-forcing is called so because it forces the ISI to zero [33]. The coefficient of the equalizer Q_n are selected for forcing the samples of the combined channel and impulse response of the equalizer to zero at all but one of the sample points that are NT spaced in the tapped delay line filter. The optimal equalizer has an associated complexity that is exponential in the channel memory length K but the beauty of the equalizer is its infinite length i.e. the number of coefficients could be increased without bound to make an infinite length equalizer with zero ISI at the receiving end.

If the time delay offered by the delay elements is equal to‘t’, then the frequency response of the equalizer $H_{eq}(f)$ has a symbol rate equal to 1/t and this response is periodic with period equal to this symbol rate. Thus satisfying the Nyquist’s first criterion, the combined frequency response of the channel and equalizer should follow the following condition in order to cancel the effect of ISI completely.

$$H_{ch}(f)H_{eq}(f)=1 \qquad :|f|<1/2t \qquad (4.5)$$

here $H_{ch}(f)$ represents the folded frequency response of the channel. The zero forcing equalizer is implemented as an inverse filter which inverts the folder frequency response of the channel.

As we know that the impulse response of a system can be stated as

$$H(z)=H_{min}(z)\ H_{AP}(z) \qquad (4.6)$$

Where, H(z)= Channel Impulse response

$H_{min}(z)$=Channel impulse response for minimum phase system

$H_{AP}(z)$=Channel impulse response for all-pass system

$|H(z)|=|H(e^{jw})|=1$

It should be remembered that the phase depends upon the placement of poles and zeroes.

At Poles: the response of the system at the poles boosts or destabilizes because of the fact that the poles are found out by the assignment of 0 value to the denominator. Figure 4.6 can best show the performance of the system with two poles at the values z=2,4

$$H1(z)=\frac{1}{(1-2z^{-1})(1-4z^{-1})} \qquad (4.7)$$

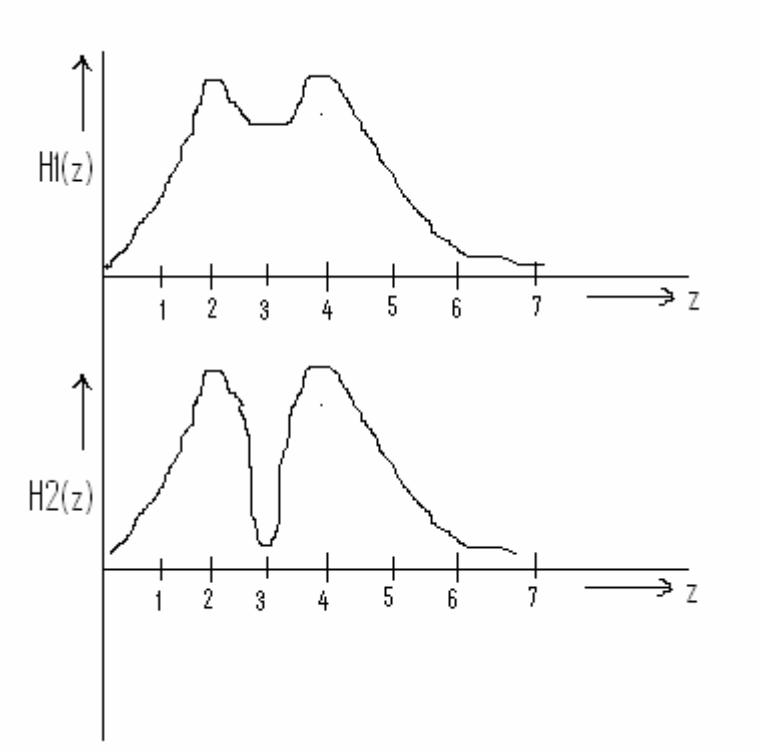

Figure 4.6: Response of the system at the poles and zeroes.

$$H2(z) = \frac{1 - 3z^{-1}}{(1 - 2z^{-1})(1 - 4z^{-1})} \tag{4.8}$$

At Zeroes: the response of the system mitigates at the zero values or the system gains stability at the zeroes value of the system. It is because of the fact that the zero values are found by assigning 0 to the numerator. Figure 4.6 shows the response of the system at the zero values z=3.

Zero forcing equalizer is a reduced complexity method for the estimation of the channel.

$$Y(z) = H(z)A(z) + N(z) \tag{4.9}$$

We can apply the zero forcing filter C(z)=1/H(z) and obtain

$$\check{Y}(z) = Y(z)C(z) = A(z) + C(z)N(z) = A(z) + \check{N}(z) \qquad (4.10)$$

It shows that the zero forcing algorithm enhances the effect of the noise alongwith the original signal as well.

When the filter C(z) is stable then all the poles lie inside the unit circle, but as the H(z) is the reciprocal of C(z) thus it follows from the stability of C(z) that all the zeros of H(z) lies inside the unit circle. And if this condition of poles and zeros is not met then Zero Forcing filter is not be applied for channel estimation and equalization.

The zero forcing equalizer was developed for wireless communication but due to noise enhancement by the inverse filter, errors are accumulated in the data and the channel is not equalized fully. Thus a combination of suitable error-correcting code with the zero forcing equalizer can enhance the performance of the system many folds. In our work we have integrated error-correcting Turbo Codes with the zero-forcing algorithm and have shown improved performance through BER curves in chapter 5.

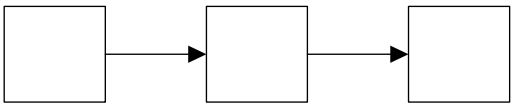

Figure 4.7: A Basic Communication Model

(b) Least-Square Error (LSE) Estimator

The essence of the Least Square Error (LSE) estimator is to estimate the system h[m] by minimizing the squared error between estimation and detection.

For the adjoined figure 4.6, the output can be written in matrix form as

$$y = xh \qquad (4.11)$$

In this equation the receiver has been taken as noiseless. If $\bar{y}$ represents the expected output then the error in the received signal is can be defined as

$$Err = \bar{y} - y \qquad (4.12)$$

The square error (SE) can be written as

$$SE = | Err |^2$$

$$SE = | \bar{y} - y |^2$$

Putting the value of y from eqtn. (4.11), we get.

$$SE = | \bar{y} - xh |^2$$

$$SE = (\bar{y} - xh)^* (\bar{y} - xh)^t \qquad (4.13)$$

Here * represents conjugate and‘t’ represents complex transpose.

Equation (4.12) can be minimized by taking the derivative w.r.t h and equating equal to zero. Thus after these mathematical manipulations the final equation that comes out is

$$h_{LS} = (x^t x)^{-1} x^t y \qquad (4.14)$$

So without requiring any prior statistical knowledge of the channel, the LS estimates are calculated with very low computational complexity.

(c) Minimum Mean Square Error (MMSE) Estimator

The MMSE estimator utilizes the second order statistics of the channel conditions to minimize the mean-square error (MSE) between the expected and received sequence which is a mean to calculate the estimator quality. Inspite of good results, extreme computational complexity prevents the use of this algorithm in the systems where trade-off between performance and computational complexity can be made.

Consider again the figure 4.6, if x is transmitted over the channel h then $y = xh$.

Again the error is given by the equation (4.12) as: Err = $\bar{y}$ - y, where $\bar{y}$ is the expected output. Now the Mean Square Error is given by the equation

Mean Square Error (MSE) = mean $\{ (\bar{y} - y)^2 \}$ = E $\{(\bar{y} - y)^2 \}$

where E is the operator for Expected value. The concept for expected value and correlation can be used to derive the equations for finding channel response. Now the auto-covariance matrices can be found as

R_{yy} = Auto-covariance matrix of 'y' $= X^{*}F^{*}R_{gg}{}^{*}F^{*'}X^{*'} + \sigma_N^2 I_N$

R_{gy} = Cross-covariance matrix of 'g' and 'y' = $R_{gg}{}^{*}\ F^{*'}X^{'}$

R_{gg} = Auto-covariance matrix of 'g'

In the above equations, σ_N^2 denotes the variance of noise and I_N represents identity matrix, both these terms alongwith R_{gg} are suppose to be known in advance. Thus the MMSE estimator is given by the equation

$$H_{mmse} = F^{*}(R_{gy}^{*}R_{yy}^{-1}y) \qquad (4.15)$$

Equation (4.15) is used for finding out MMSE estimate for both SISO and MIMO systems. In the low SNR scenarios, MMSE estimator has a better performance than LSE estimator. But the major drawback of MMSE estimator is the high computational complexity, which prevents its usage. LSE estimation alongwith a good error-correcting codes can perform better than MMSE estimator in the Rayleigh fading environment.

4.4.1.2 Comb-type Channel Estimation

Figure 4.5(b) shows a schematic view of the comb-type pilot insertion technique. This technique is used in the fast fading environments in which

the channel impulse response is varying inside an OFDM data block. So system requires channel tracking, alongwith estimation. This is done with the help of comb-type pilot insertion technique.

In this technique a few of the subcarriers inside the OFDM symbols are dedicated for pilot tones. No dedicated symbols are used for pilot data insertion. Thus all the OFDM symbols contain a few subcarrier containing pilot data. This allows fast tracking of the varying channel impulse response.

Estimation is based on the three algorithms that we have explained for block-type case. But in comb-type pilot assisted channel estimation, an additional step has to be taken after estimation, and this step is interpolation of the channel. After getting estimates of the channel at the pilot subcarrier locations, the channel impulse response is calculated through interpolation in between the two pilot subcarriers. Interpolation refers to the process of making calculated guess about the value of a variable from an incomplete set of values by looking at the general trend of the variation. Some of the important and generally used interpolation techniques include Linear Interpolation, Second-Order Interpolation, Low-Pass Interpolation, Spline Cubic Interpolation etc.

4.4.2 Non-Pilot Assisted (Blind) Channel Estimation

In some cases the use of training sequence is either impractical or not feasible due to the scarce of bandwidth. In such case the channel is estimated in the absence of pilot sequence and this process is termed as blind channel estimation/identification.

In order for blind channel estimation to be possible, some prior knowledge of the channel and the transmitted data is required. This knowledge involves distribution of the transmitted signal, the relative duration of the signal and the channel impulse response and the stationary or time-varying nature of the signal and the channel [34].

The only advantage that blind channel estimation has is the efficient utilization of bandwidth by cutting off the overhead used by the pilot tones so it is excellent for the applications where bandwidth is scarce. Otherwise extremely high computational complexity and requirement of prior knowledge of mathematical properties of the channel and signal makes it difficult to implement on the real systems.

4.5 Conclusion

In this chapter we have introduced the channel estimation and equalization technique used by us in the proposed system of OFDM. The chapter starts with an introduction to wireless channel and its different characteristics that affect the quality of the signal. After this, light is put on different types of channel estimation and equalization techniques that include pilot-assisted and non pilot-assisted strategies. There uses in different scenarios have been discussed. Following this, classifications of pilot-assisted channel estimation technique based on the pilot tone insertion method is discussed alongwith its effectiveness in different environments. Similarly an introduction is given to the different algorithms which can be used to implement these techniques with a comparision amongst them. After making comparisons, frequency-domain pilot-assisted block-type Channel Estimation method has been chosen to be implemented in the proposed system due to its effectiveness.

Chapter-5

IMPLEMENTATION AND SIMULATION RESULTS

5.1 Introduction

In this chapter, results of the proposed model of OFDM have been shown through MATLAB simulation with different modulation schemes and through various channels. First of all, the frame format suggested for sending data of the simulated model is shown and then light is put on the parameters and the methodology used for channel estimation and equalization of the proposed system. Simulation results have been given for different modulation schemes like BPSK, QPSK, 16-QAM and 64-QAM and are compared. The results of the turbo decoder have been shown for different number of iterations. In the final portion of the chapter conclusions have been made regarding the best choice.

5.2 Frame Format and System Parameters

The channel estimation algorithm used by us is Frequency-domain pilot-assisted block-type zero forcing technique. In this procedure, a pilot OFDM symbol is transmitted prior to the data symbols and depending upon the impairments introduced in the pilot symbol, channel is estimated for the upcoming data symbols.

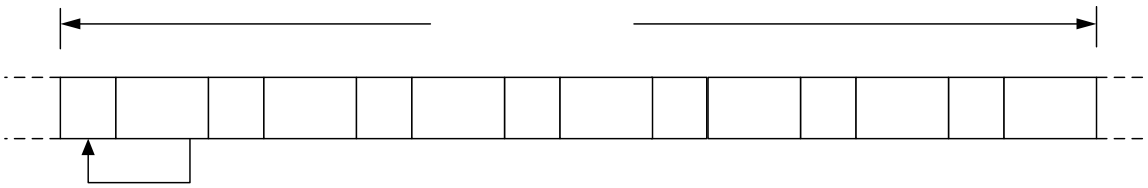

CP= Cyclic Prefix, CEB=Channel Estimation Block, DB=Data Block

Figure 5.1: Formation of Frame Unit for the simulated OFDM transmission

One frame consists of seven blocks of data, out of which first block is the pilot symbol block and the rest of the six are information data symbols. Depending upon the channel estimated by the pilot symbol, equalization is done for the upcoming six data symbol. The frame format is shown in figure 5.1. Each OFDM symbol is comprised of 512 subcarriers for BPSK, QPSK and 256 subcarriers for 16-QAM, 64-QAM and the length of the cyclic prefix is kept ¼ otherwise mentioned.

Each block of information data symbols as well as pilot data symbols consists of 1kbits otherwise mentioned. So the length of one frame unit comes out to be 7 kbits with a pilot data overhead of 1 kbits. Thus the overall overhead in terms of channel estimation pilot symbols comes out to be approx. 14%. The size of the FFT is 512 for BPSK, QPSK and 256 for 16-QAM and 64-QAM. The combination of channel estimation with parallel concatenation and recursive decoding scheme allows improving the

performance of the proposed model in comparison with the already published work in this area.

5.3 OFDM with Channel Estimation

Under this topic the performance of the OFDM system with frequency-domain Pilot-assisted Block-Type Channel Estimation will be discussed with different modulation schemes.

Figure 5.2 shows the performance of the proposed system with 64-QAM modulation scheme. OFDM symbol comprises 256 subcarriers and the size of the cyclic prefix is 64. The size of one OFDM Symbol is 1.5kbits and the size of one frame unit as depicted in figure 5.1 is 9Kbits(information data).

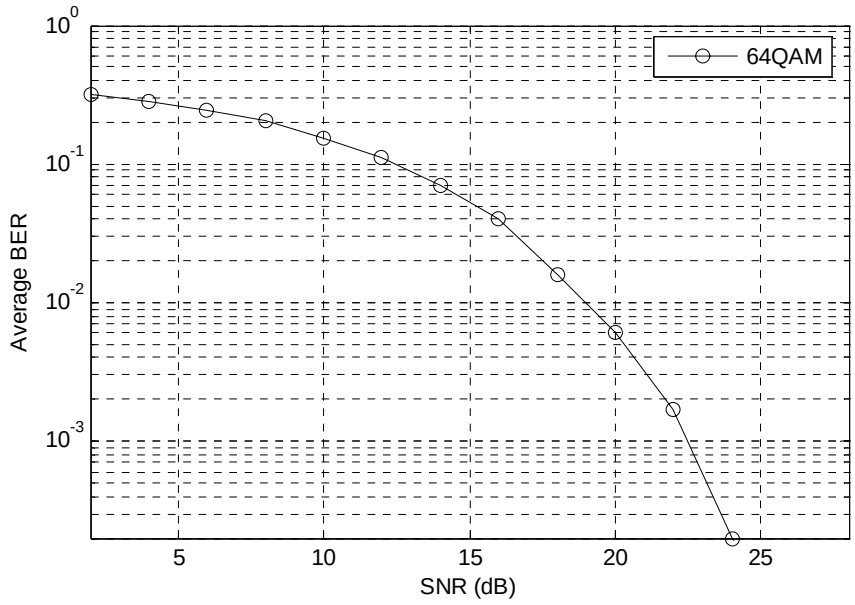

Figure 5.2: BER Curve of OFDM system for 64-QAM with Block-type Channel Estimation in AWGN environment

The above result shows that the SNR threshold value for 64-QAM is 24dB for 10e-3 BER. These results are taken on AWGN channel. The same parameters when applied to 16-QAM, QPSK and BPSK produce the following results.

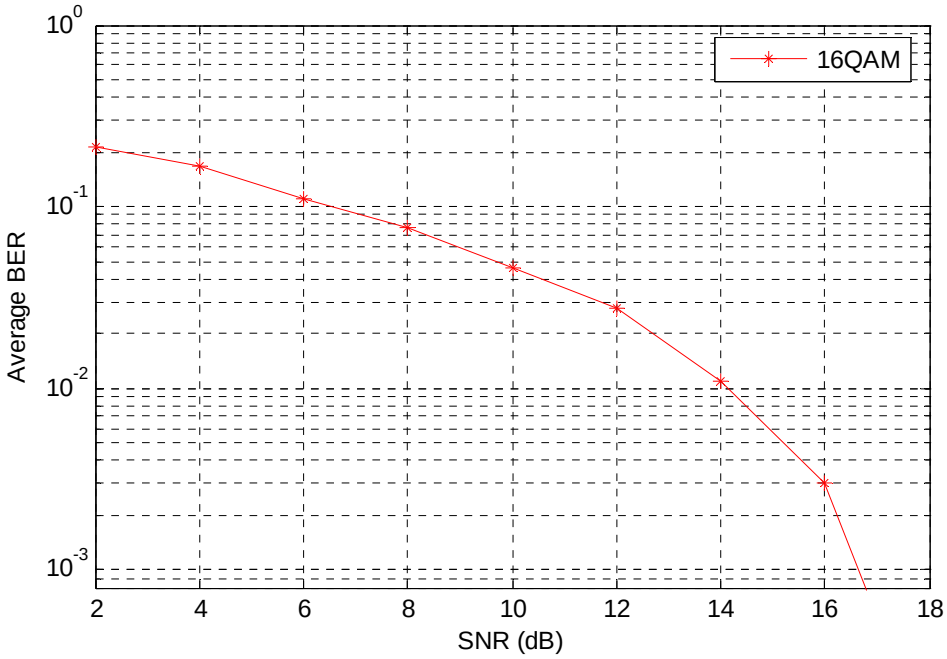

Figure 5.3: BER Curve of OFDM system with block-type Channel Estimation for 16-QAM in AWGN environment

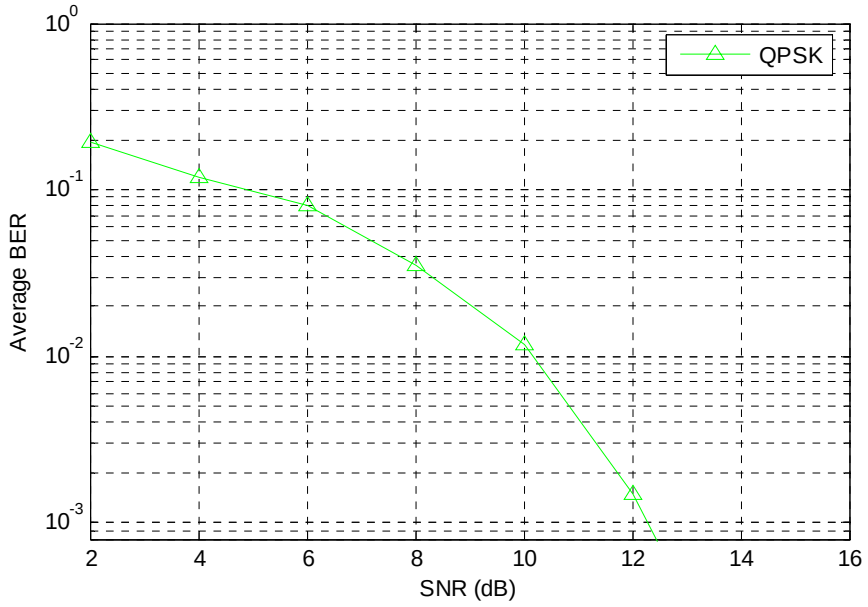

Figure 5.4: BER Curve of OFDM system with Channel Estimation for QPSK in AWGN environment

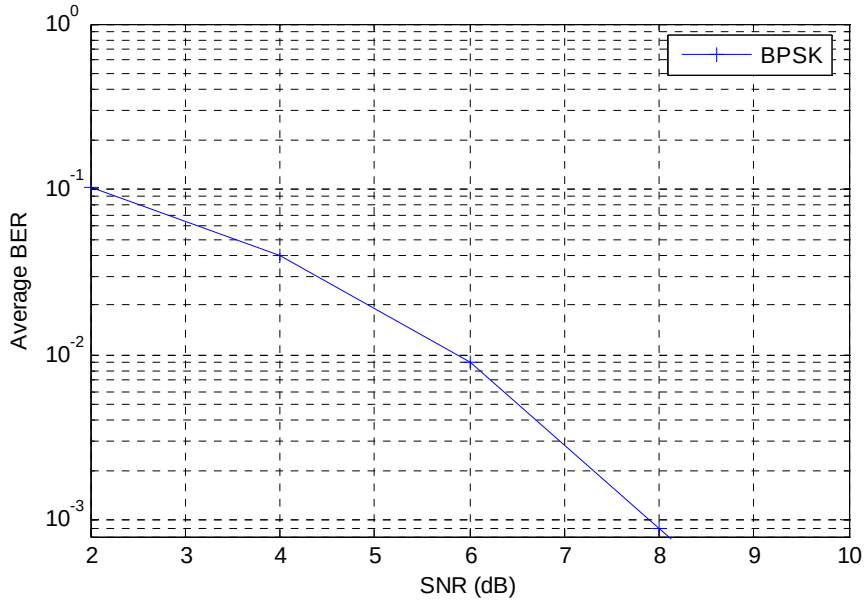

Figure 5.5: BER Curve of OFDM system with Channel Estimation for BPSK in AWGN environment

The above figures show the BER curves of OFDM with pilot assisted block-type channel estimation for different modulation schemes in AWGN environment. On the x-axis is Signal to Noise Ratio and on the Y-axis is BER. The results show that the lower modulation schemes exhibit low BER as compared to the higher modulation schemes for same signal power. It is justified theoretically from the fact that the lower modulation schemes have symbols mapped much apart on the constellation diagram so there are very less chances for the symbols to interfere during the course of transmission. Ideally BPSK symbols are 180° apart while 64-QAM symbols are 12.8571° apart (squared constellation considered). Thus the chances of interference amongst the symbols of BPSK is less as compared to 64-QAM. The SNR threshold value for 10e-3 for the four modulation schemes in AWGN channel is 8.1dB, 12.2dB, 16.8dB and 24dB for BPSK, QPSK, 16-QAM and 64-QAM respectively.

Figure 5.6 shows the comparison curve of the different modulation schemes on the same scale. The curve depicts a BER improvement for lower order modulation schemes but this BER improvement for lower modulation schemes is achieved at the expense of data rate that is compromised by the usage of lower modulation schemes. So depending

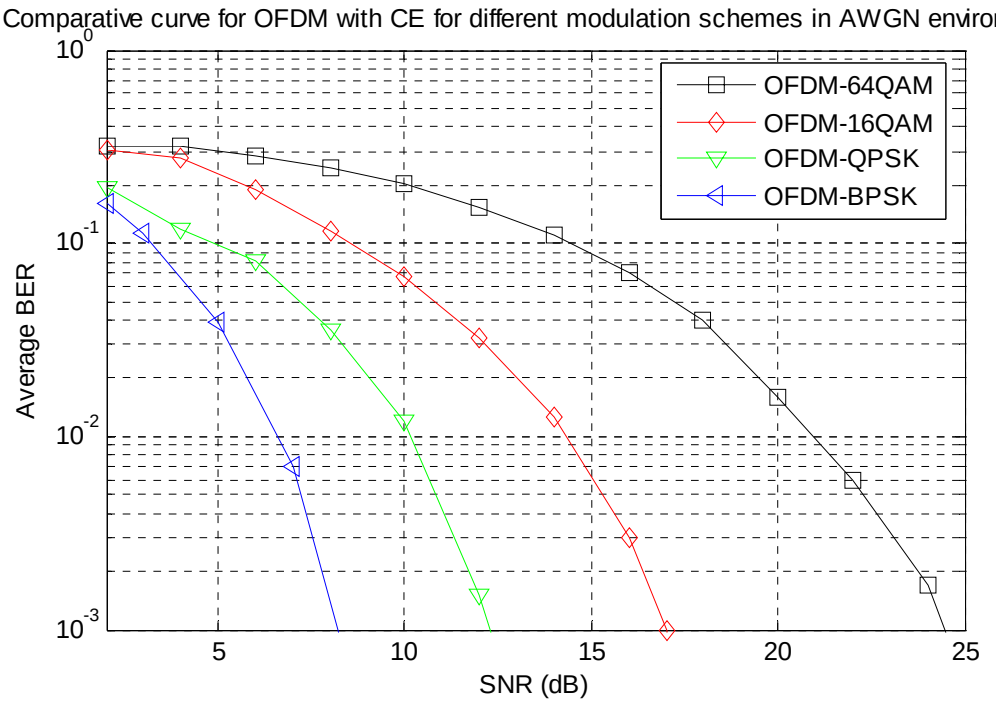

Figure 5.6: BER Curve for OFDM system with Channel Estimation for different modulation schemes in AWGN environment

upon the application for which the system is designed one has to choose a modulation scheme that 'ld make a trade-off between the tolerable error rate and required data rate.

5.4 Turbo-Coded OFDM with Channel Estimation

Turbo Codes have been incorporated in proposed model of OFDM shown in figure 5.7 with MAP decoding algorithm at the receiver side and the performance has been analyzed with 1, 2, 4, 8 and 20 numbers of iterations for different modulation schemes. At the transmitting side we have used a

Turbo Code Encoder using two ½ rate Recursive Systematic Convolutional (RSC) Encoders that are discussed in detail in Sec. 3.2.

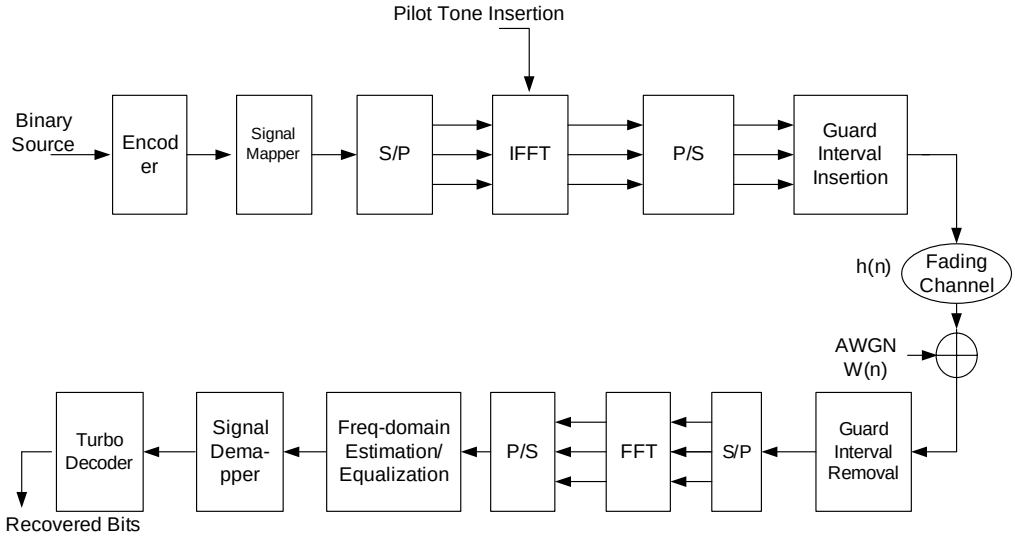

Figure 5.7: Simulated Turbo-Coded OFDM System with Frequency-domain Estimation and Equalization

The two RSC encoders encode the information sequence twice with the encoded sequences statistically independent due to the presence of Random interleaver in between the two encoders. This interleaver has been discussed in detail in Sec. 3.4.3.

The decoder comprises two component MAP decoders serially concatenated via an interleaver. Each of the component MAP Decoder exchanges soft information with the other component MAP Decoder to improve the a-priori probability. After a fixed number of iterations hard decision is made on the extrinsic information to decide for a bit 1 or 0.

First of all a comparison is made for Turbo-Coded OFDM system with different modulation schemes in AWGN channel and the results are compared amongst eachother and with the performance curves obtained in section 5.3, figure 5.6. The obtained results with the error correcting turbo codes show a clear performance improvement when compared with the previously obtained results of section 5.3. The frame format and parameters like length of cyclic prefix etc are kept constant for both. BER curve for BPSK, QPSK, 16-QAM and 64-QAM are shown below.

Figure 5.8 shows the BER performance curve for Turbo-Coded OFDM system with BPSK modulation for 20 iterations with Pilot-assisted Block-type Channel estimation in AWGN Channel. This curve when compared with the curve of figure 5.5, shows a performance improvement of almost 2.1 dB which is due to the implementation of error correcting turbo codes.

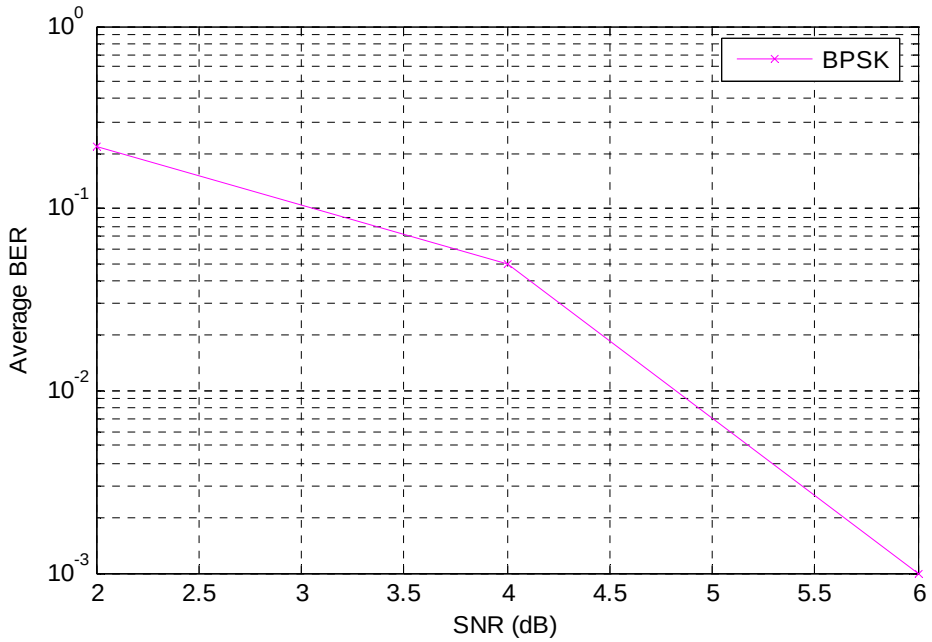

Figure 5.8: BER Curve for Turbo-Coded OFDM System with Channel Estimation for BPSK in AWGN environment

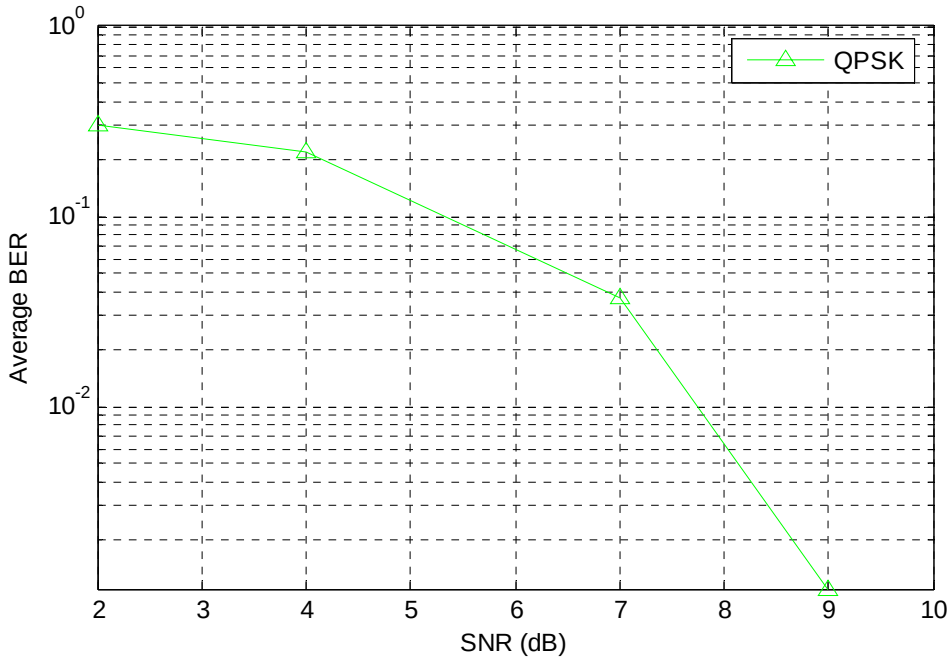

Figure 5.9: BER Curve for Turbo-Coded OFDM System with Channel Estimation for QPSK in AWGN environment

Figure 5.9 shows the BER curve for Turbo-Coded OFDM system with channel estimation for 20 iterations of MAP decoder for QPSK modulation in AWGN channel. This performance curve when matched with the curve of figure 5.4 shows a performance improvement of almost 3.2 dB which is due to the implementation of Turbo-codes. Frame format and all the other parameter of the two systems were kept the same.

Figure 5.10 shows the BER curve for turbo-coded OFDM System for 20 iterations with block-type pilot-assisted channel estimation for 16-QAM modulation scheme. When compared with figure 5.3 shows a performance gain of almost 2.8 dB over the system that has been simulated under the same environment without Turbo Codes. So it shows

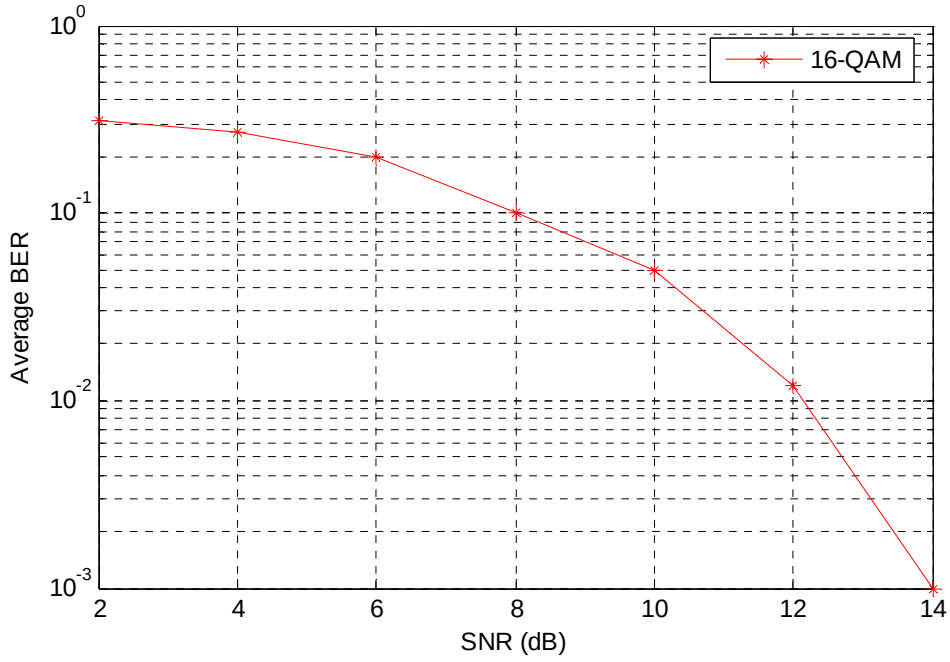

Figure 5.10: BER Curve for Turbo-Coded OFDM System with Channel Estimation for 16-QAM in AWGN environment

that a small computational complexity introduction into the system in the form of Turbo codes have improved the performance of the system to much extent.

Figure 5.11 shows BER curve for turbo-coded OFDM system with pilot-assisted block type channel estimation for 64-QAM modulation scheme with 20 iterations of the MAP decoder in AWGN environment. The curve when compared with the curve of figure 5.2 shows a SNR gain of almost 6 dB in the same environment and under the same communication parameters.

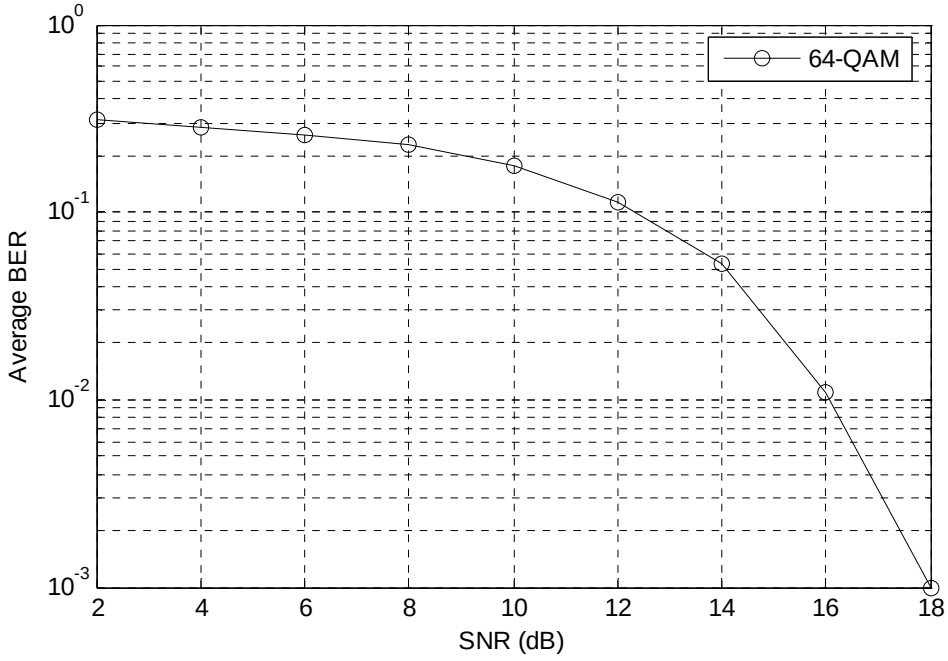

Figure 5.11: BER Curve for Turbo-Coded OFDM System with Channel Estimation for 64-QAM in AWGN environment

Figure 5.12 shows the cumulative performance comparison of the above four modulation schemes in AWGN environment and shows the performance improvement as we move to the lower order modulation schemes. This is because of the geometry of constellation mapping of the information symbols. For squared constellation, mapped symbols are 180°, 90°, 30° and 12.857° apart from each other for BPSK, QPSK, 16-QAM and 64-QAM respectively. So moving towards higher order modulation schemes increases the chances of interference amongst the modulated information

symbols which is also depicted from the performance curves. As discussed earlier, the choice of the modulation

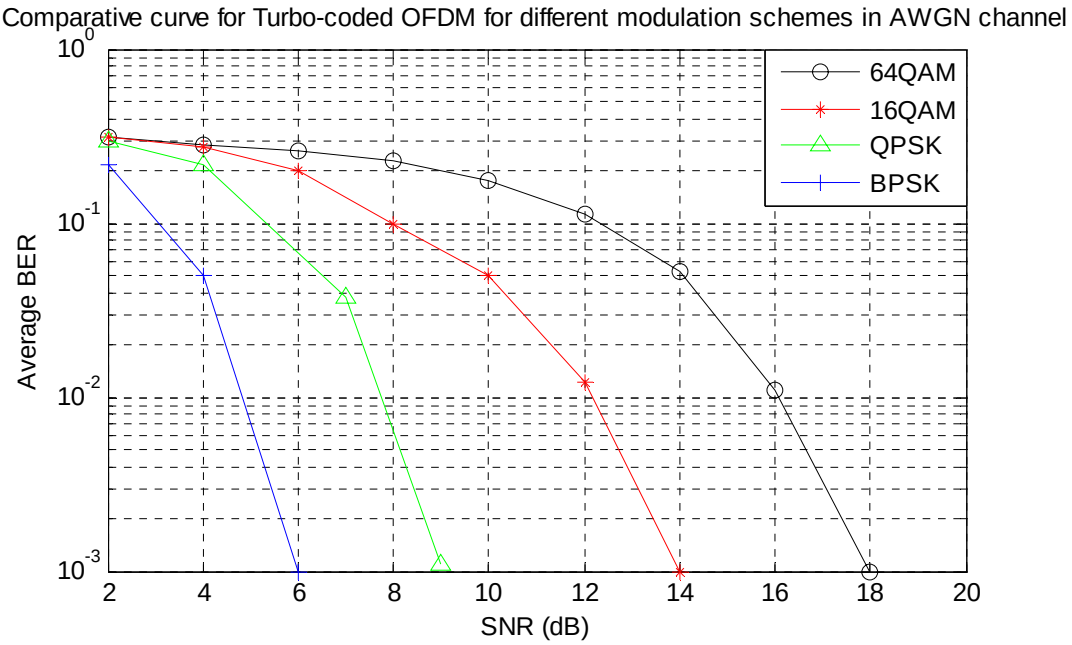

Figure 5.12: BER Curve of different modulation schemes for turbo-coded OFDM system with Channel Estimation in AWGN environment

scheme depends upon the trade-off between data rate and the performance gain that is required by the system to run the application it is designed for.

5.5 Results with multi-iterations of Turbo MAP Decoder:

In the following lines, the performance of the proposed OFDM system has been given for different number of iterations of MAP decoder for the four modulation schemes. In the succeeding figures the information symbols have been passed through the Rayleigh fading AWGN channel. The BER

performance of BPSK with 1, 2, 4, 8 and 20 numbers of iterations is given below.

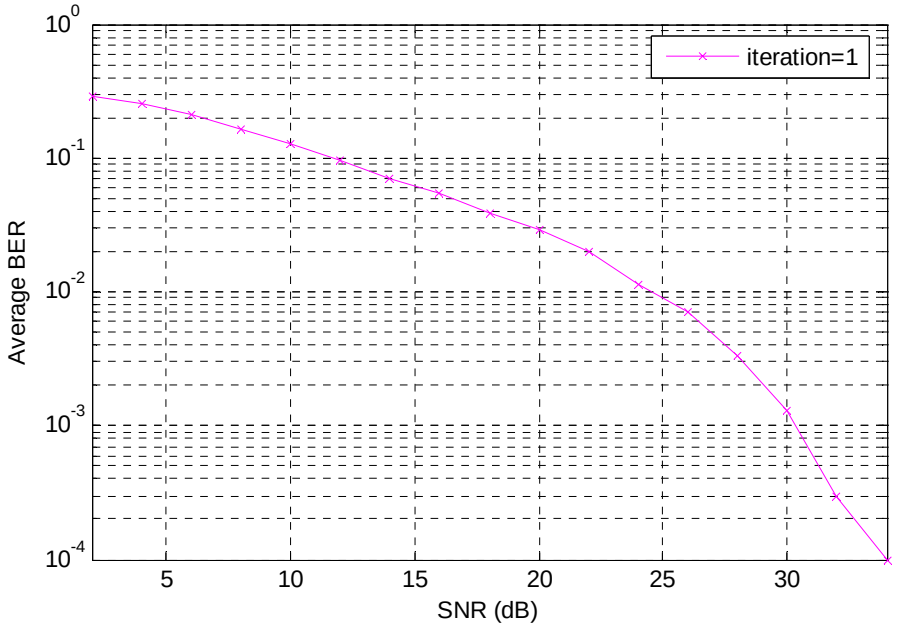

Figure 5.13: BER Curve of Turbo-Coded OFDM with Channel Estimation for BPSK modulation scheme on Rayleigh fading AWGN channel for one iteration of MAP Decoder

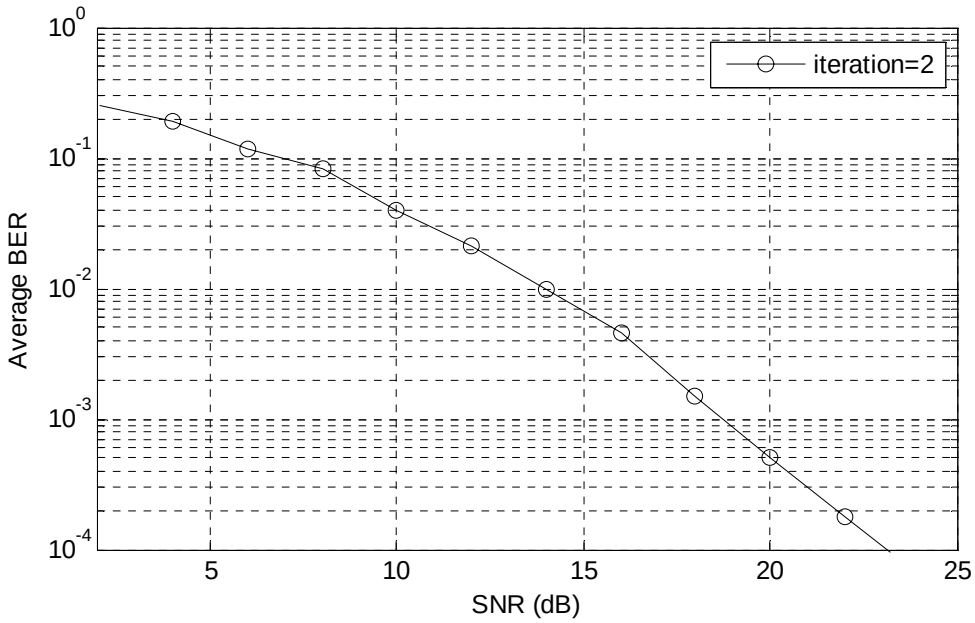

Figure 5.14: BER Curve of Turbo-Coded OFDM with Channel Estimation for BPSK modulation scheme on Rayleigh fading AWGN channel for two iterations of MAP Decoder

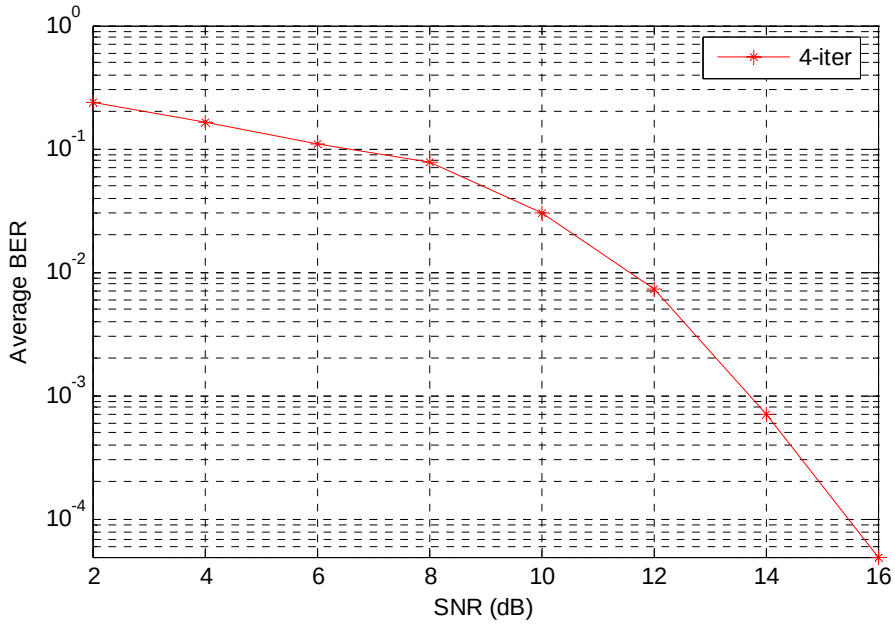

Figure 5.15: BER Curve of Turbo-Coded OFDM with Channel Estimation for BPSK modulation scheme on Rayleigh fading AWGN channel for 4 iterations of MAP Decoder

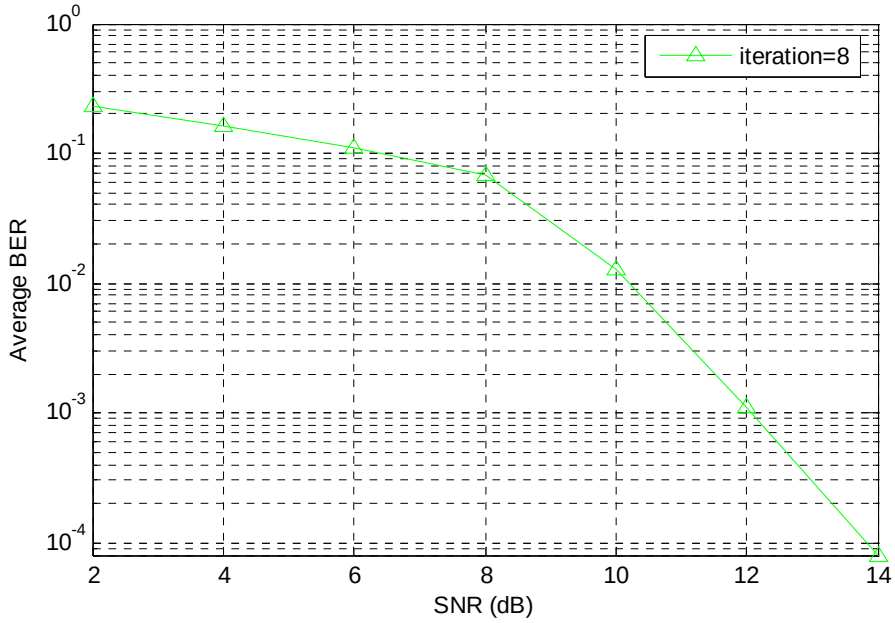

Figure 5.16: BER Curve of Turbo-Coded OFDM with Channel Estimation for BPSK modulation scheme on Rayleigh fading AWGN channel for 8 iterations of MAP Decoder

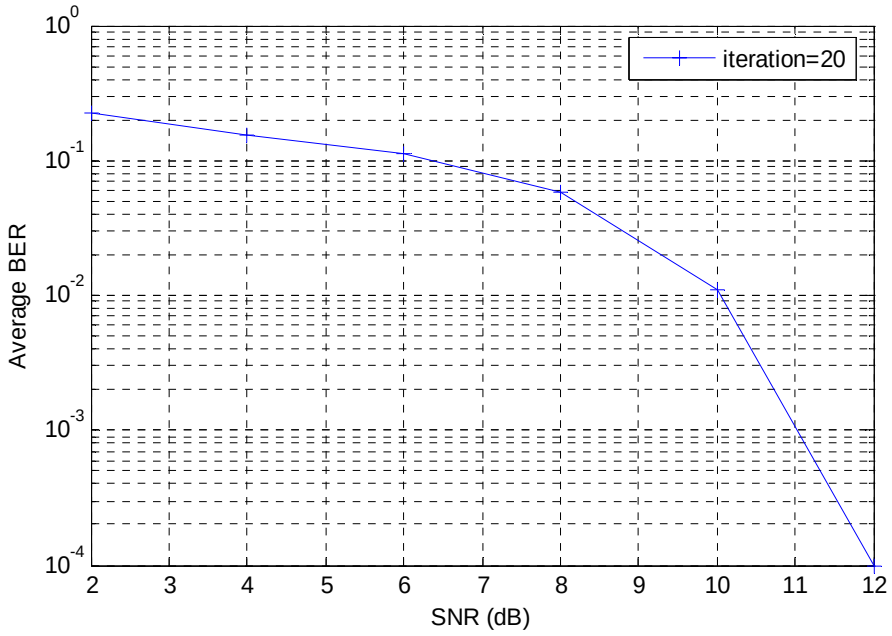

Figure 5.17: BER Curve of Turbo-Coded OFDM with Channel Estimation for BPSK modulation scheme on Rayleigh fading AWGN channel for 20 iterations of MAP Decoder

The results shown in figure 5.13-5.17 for the simulated system illustrates that the performance of the Turbo-Coded OFDM system improves with increasing number of iterations of MAP decoder. It is shown that the performance improves abruptly as the system moves from 1 iteration to 2 iterations but the performance improvement decreases gradually as the number of iterations increases further with a large computational complexity introduction to the system. Reason lies in the diversion of the LLR value (eqtn. 3.3) from mean 0 to the extent that the system reaches an almost stable state and any further iteration improves the coding gain very less. So

one has to make a compromise between the computational complexity that system can afford and the required coding gain. Increasing computational complexity enhances the system latency which in turn prevents the system to be used for many real-time applications.

Figure 5.18 shows a comparative graph of the different number of iterations for BPSK with Block-type channel estimation in Rayleigh fading environment with AWGN noise added at the receiver. The graph is showing decreasing coding gain as the numbers of iterations are increased. The cumulative performance curve when compared with figure 5.12 shows a performance degradation of 5.5 dB due to the presence of Rayleigh fading in the channel. Figure 5.12 shows a BER performance

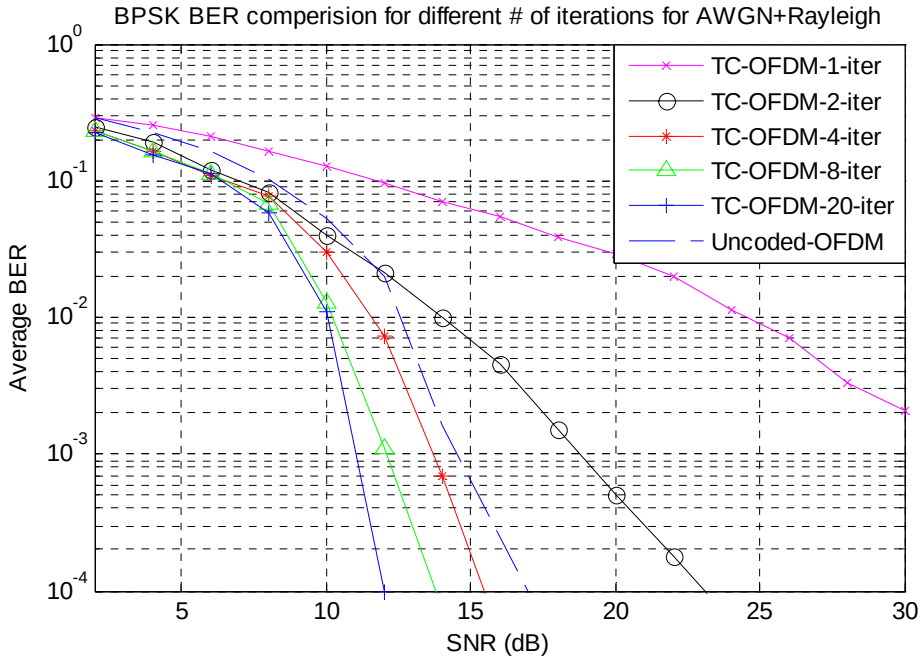

Figure 5.18: Comparison curve of Turbo-Coded OFDM with Channel Estimation for BPSK modulation for 1,2,4,8 and 20 iterations of MAP decoder for Rayleigh fading AWGN channel

of 10e-3 at an SNR of 6dB by the application of 20 iterations of MAP decoder. But the same parameters when applied to the proposed system in the presence of Rayleigh fading environment shows the achievement of 10e-3 at the SNR of almost 11.5 dB (figure 5.18). So a degradation of 5.5 dB goes to the credit of Rayleigh distributed fading.

In the following lines the BER performance of the OFDM system with QPSK modulation for different number of iterations of MAP decoder has been shown. This performance is found to be degraded as compared to the performance of BPSK under the same environment because of the close constellation mapping (90° vs 180°) of the symbols. This close mapping originates a possibility for the OFDM symbols to be corrupted during the course of transmission through the Rayleigh fading channel which is depicted in the BER performance curve. But the data rate of the QPSK is twice as that of the BPSK modulation scheme due to the mapping of two bits/symbol compared to 1 bit/symbol in the case of BPSK. The BER performance curves for 1, 2, 4, 8 and 20 number of iterations are shown in the following figures.

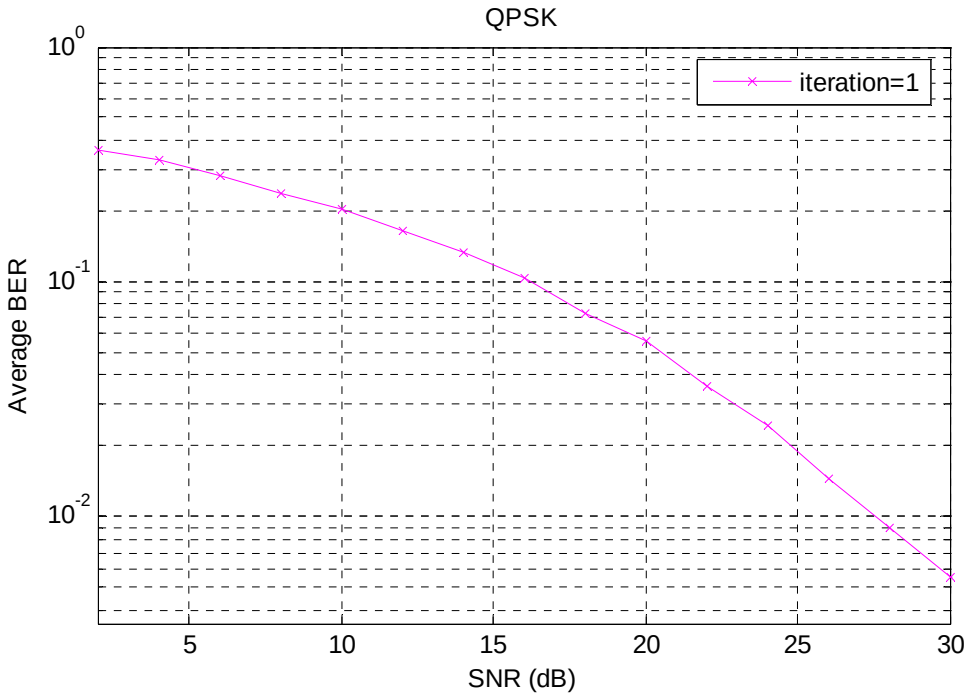

Figure 5.19: BER Curve of Turbo-Coded OFDM with Channel Estimation for QPSK modulation scheme on Rayleigh fading AWGN channel for single iteration of MAP Decoder

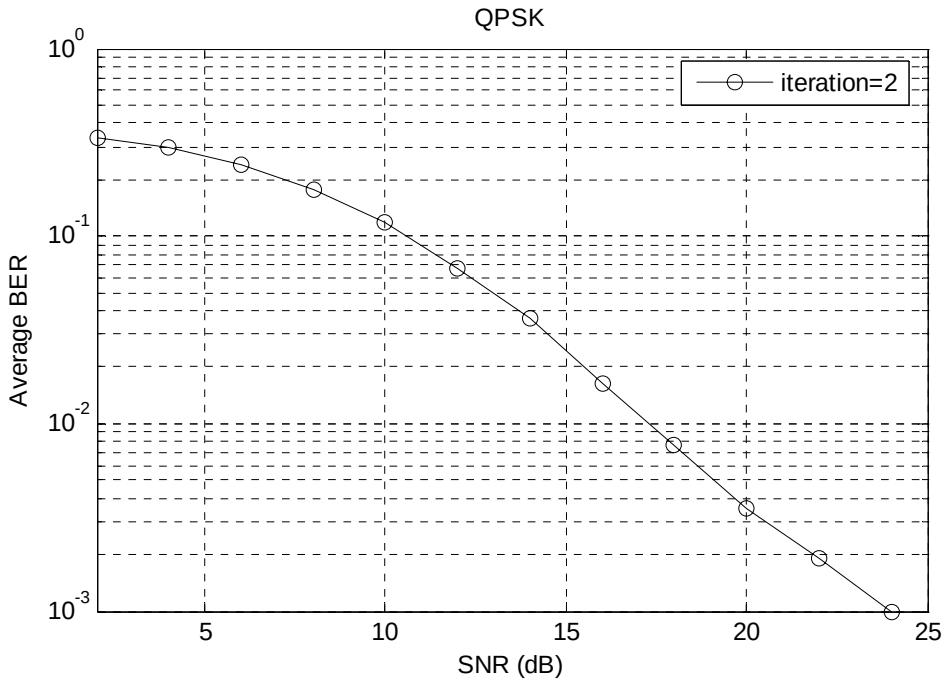

Figure 5.20: BER Curve of Turbo-Coded OFDM with Channel Estimation for QPSK modulation scheme on Rayleigh fading AWGN channel for 2 iterations of MAP Decoder

Figure 5.19 and 5.20 shows the performance of turbo coded OFDM with QPSK modulation scheme in Rayleigh fading environment for 1 and 2 iterations of MAP decoder. The two figures show an abrupt improvement of the performance as the iterations has been increased from 1 to 2. The succeeding figures show that the performance improvement is less for further increase in the number of iterations. As discussed in the BPSK case, this is due to the diversion of the LLR from the mean 0 to the extent that the system reaches a stable state. The performance graphs for 4, 8 and 20 iterations are given in figure 5.21-5.23.

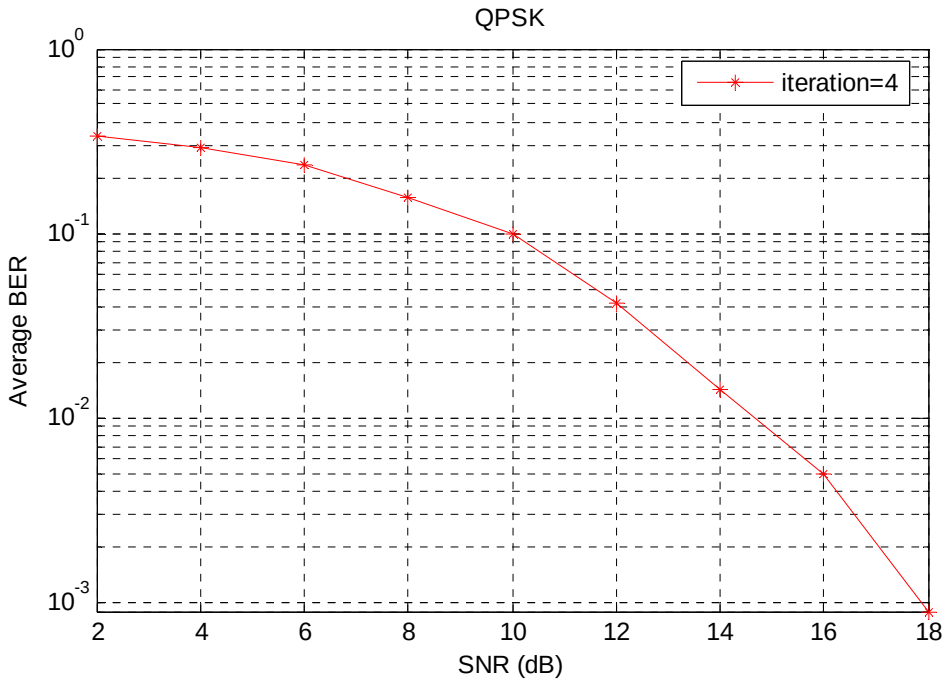

Figure 5.21: BER Curve of Turbo-Coded OFDM with Channel Estimation for QPSK modulation scheme on Rayleigh fading AWGN channel for 4 iterations of MAP Decoder

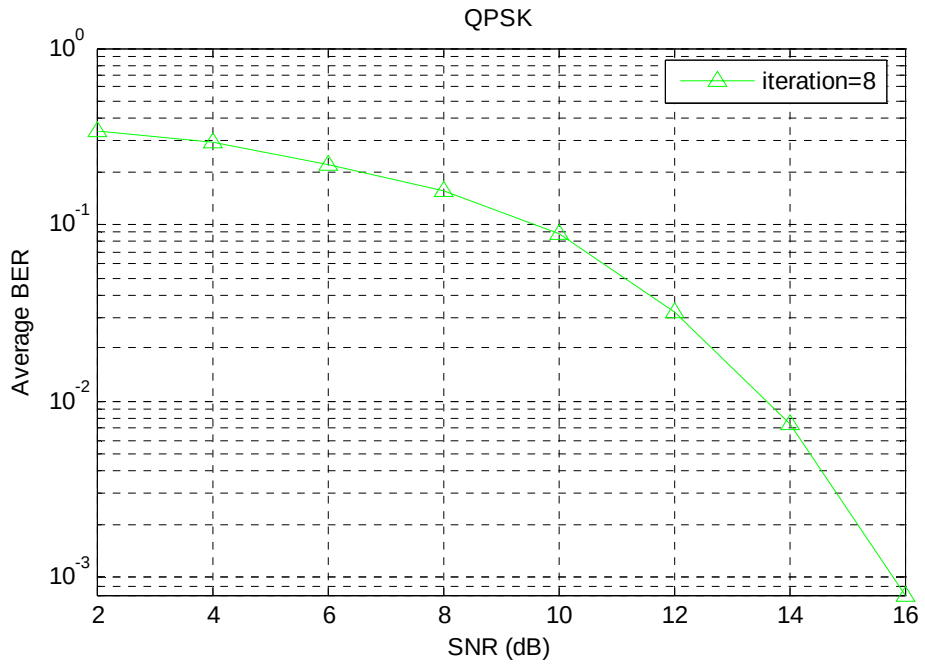

Figure 5.22: BER Curve of Turbo-Coded OFDM with Channel Estimation for QPSK modulation scheme on Rayleigh fading AWGN channel for 8 iterations of MAP Decoder

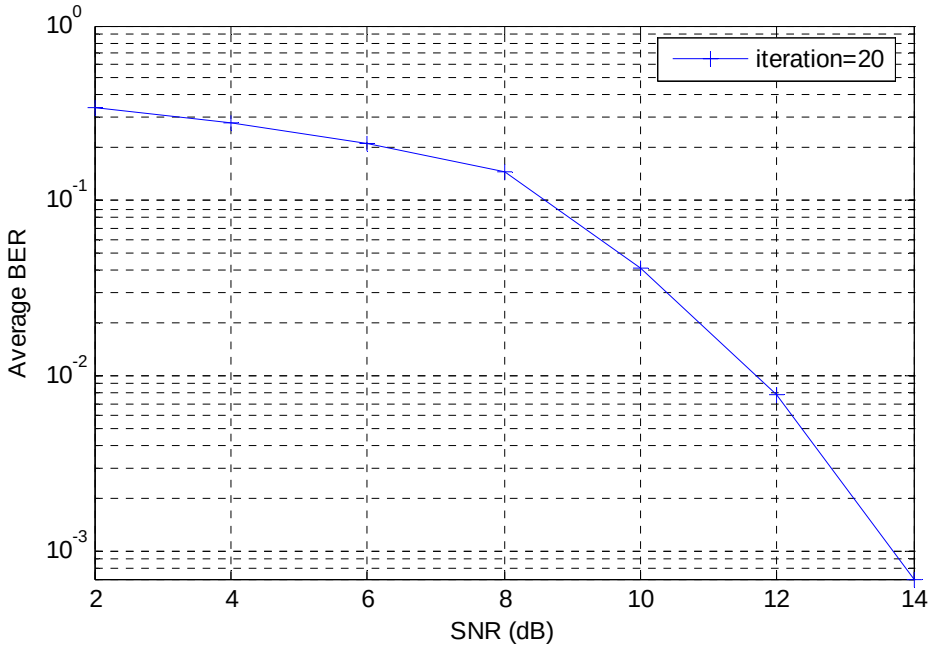

Figure 5.23: BER Curve of Turbo-Coded OFDM with Channel Estimation for QPSK modulation scheme on Rayleigh fading AWGN channel for 20 iterations of MAP Decoder

The comparative performance curve for 1, 2, 4, 8 and 20 iterations of MAP decoder with QPSK modulation scheme for the presented OFDM system on the same scale is given in figure 5.24. The curve shows the coding gain achieved by the turbo-coded OFDM system by increasing the number of iterations of MAP decoder.

The comparative performance graph for turbo-coded OFDM with QPSK modulation scheme when compared with figure 5.12 shows a performance degradation of almost 5dB. This is because of the presence of Rayleigh distributed fading in the environment through which the signal is passed.

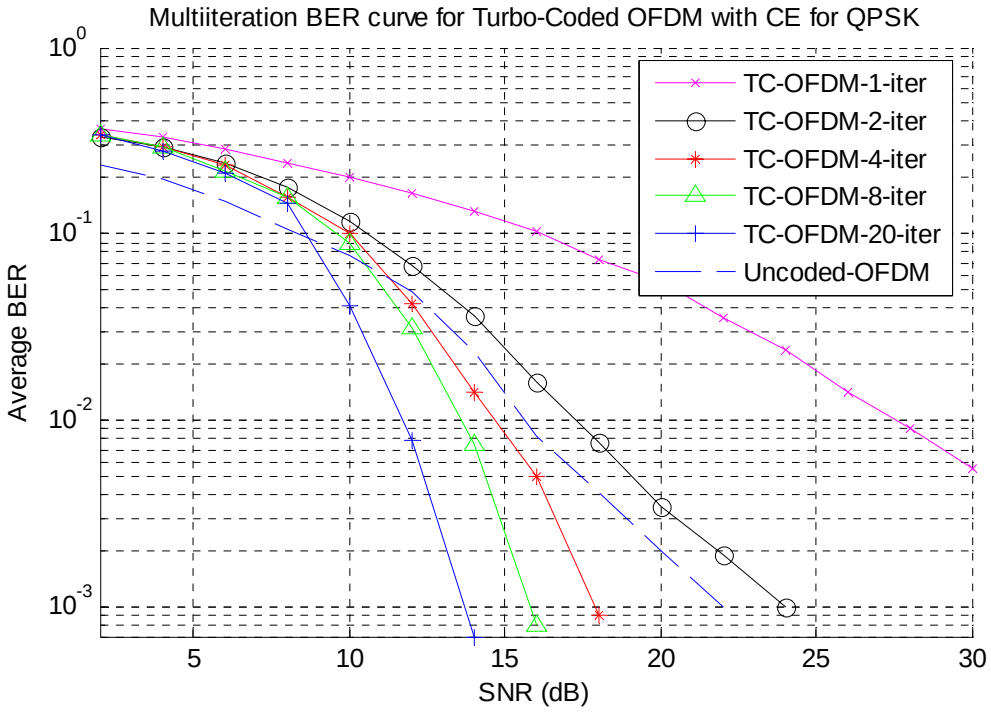

Figure 5.24: Comparison curve of Turbo-Coded OFDM with Channel Estimation for QPSK modulation for 1,2,4,8 and 20 iterations of MAP decoder in Rayleigh fading AWGN channel

In the upcoming figures performance curves have been shown for comparatively higher modulation schemes like 16-QAM and 64-QAM. The OFDM symbol comprises 256 subcarriers for 16-QAM and the size of the

cyclic prefix is 64. 1/3 rate encoder is used at the transmitter end which is comprised of two ½ rate Recursive Systematic Convolutional (RSC) Encoders explained in section 3.2. MAP decoding algorithm is used at the Receiver side and the BER performance curves are shown for 1, 2, 4, 8 and 20 iterations.

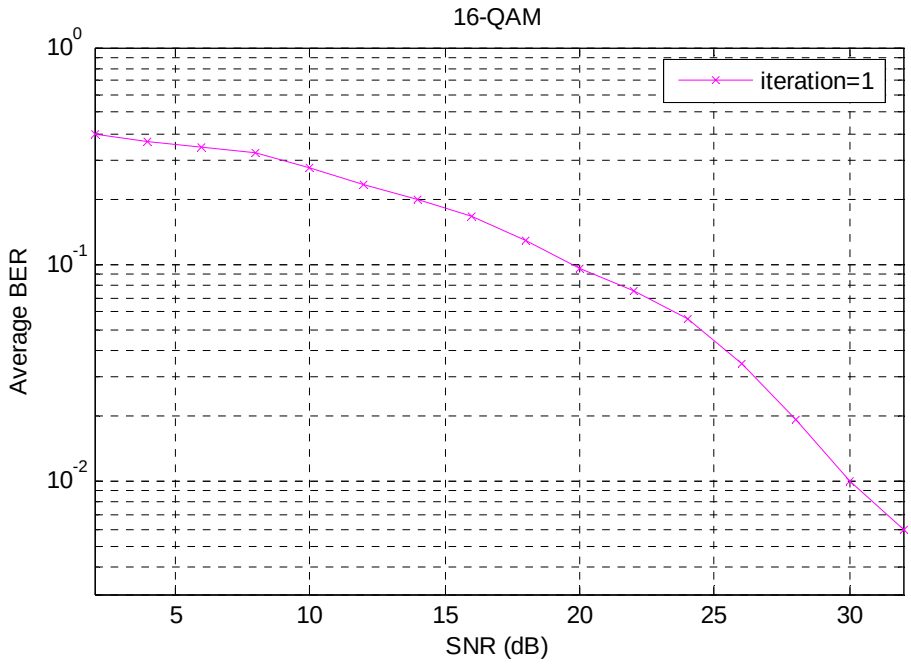

Figure 5.25: BER Curve of Turbo-Coded OFDM with Channel Estimation for 16-QAM modulation scheme on Rayleigh fading AWGN channel for single iteration of MAP Decoder

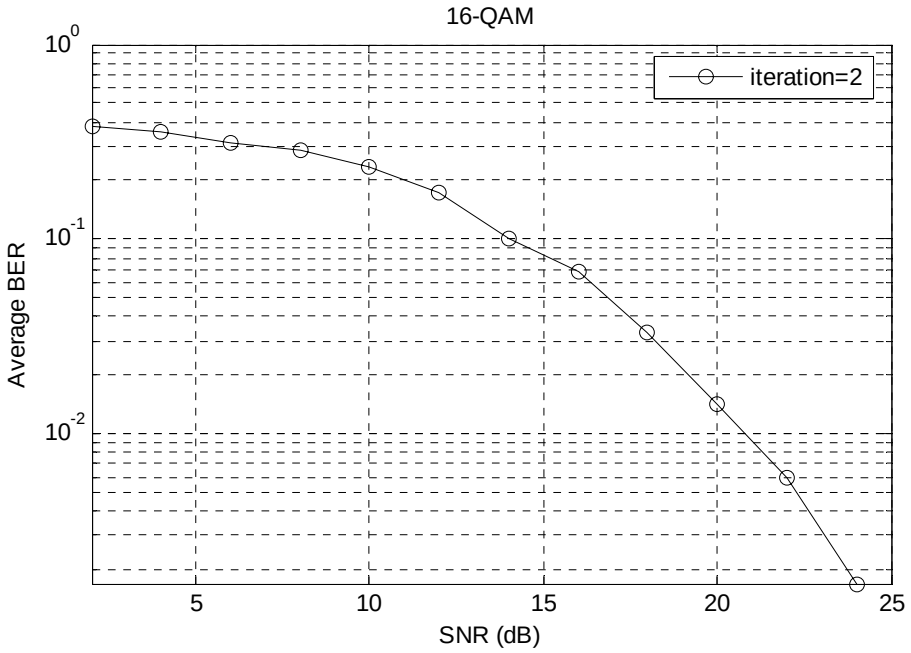

Figure 5.26: BER Curve of Turbo-Coded OFDM with Channel Estimation for 16-QAM modulation scheme on Rayleigh fading AWGN channel for two iterations of MAP Decoder

Figure 5.25 and figure 5.26 shows an abrupt coding gain for a bit error rate in the range of 10e-2 to 10e-3. But this coding gain drops gradually as the numbers of iterations are increased further because of the diversion of the LLR from the mean 0. This is depicted in figure 5.27 to 5.29.

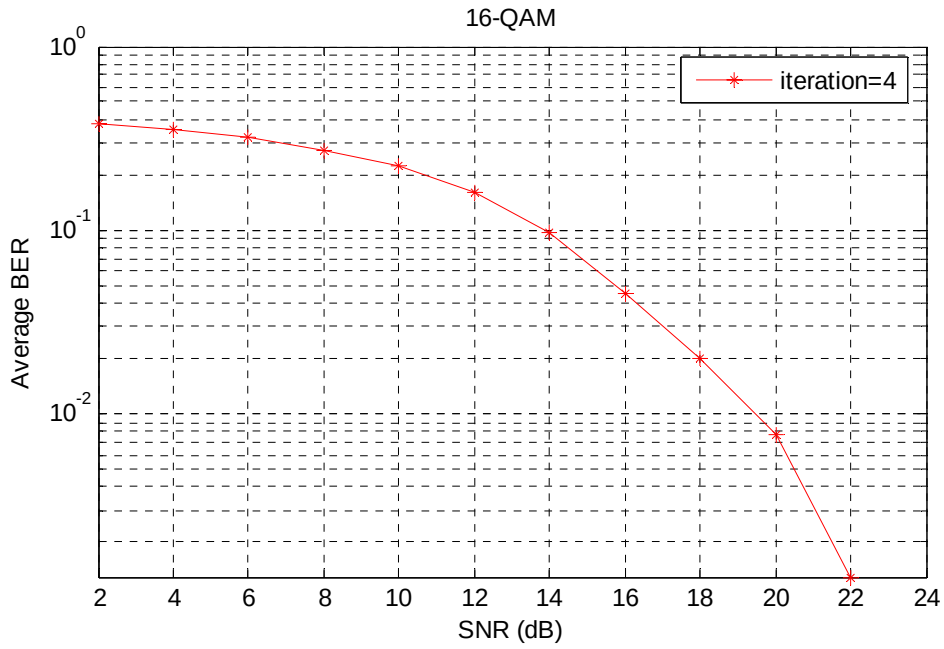

Figure 5.27: BER Curve of Turbo-Coded OFDM with Channel Estimation for 16-QAM modulation scheme on Rayleigh fading AWGN channel for 4 iterations of MAP Decoder

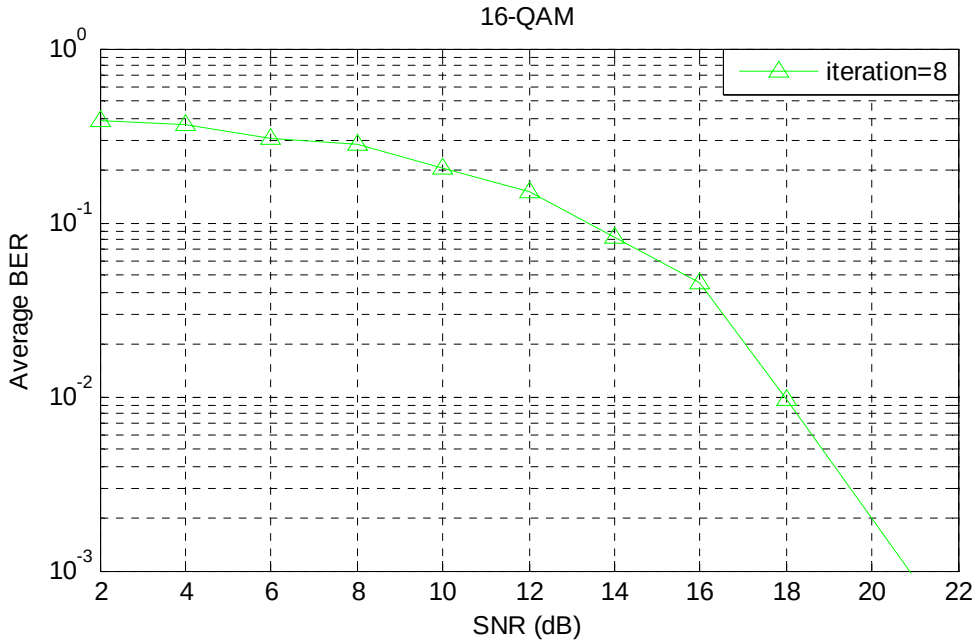

Figure 5.28: BER Curve of Turbo-Coded OFDM with Channel Estimation for 16-QAM modulation scheme on Rayleigh fading AWGN channel for 8 iterations of MAP Decoder

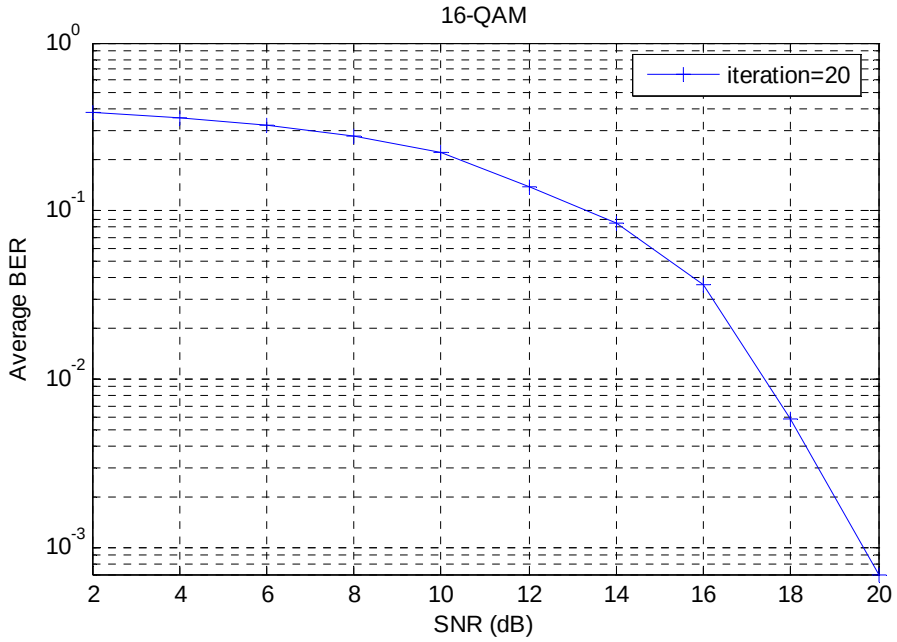

Figure 5.29: BER Curve of Turbo-Coded OFDM with Channel Estimation for 16-QAM modulation scheme on Rayleigh fading AWGN channel for 20 iterations of MAP Decoder

Figure 5.29 when compared with figure 5.12 shows a performance degradation of almost 6dB at the bit error rate of 10e-3 due to the presence of Rayleigh distributed fading in the channel.

The cumulative multi-iteration comparative performance curve, collectively showing the performance of the proposed system with different number of iterations of MAP decoder is shown in figure 5.30. Again the

performance curve shows that the coding gain is high as the number of iteration is increased from 1 to 2 but for further increase in the number of iterations the coding gain drops.

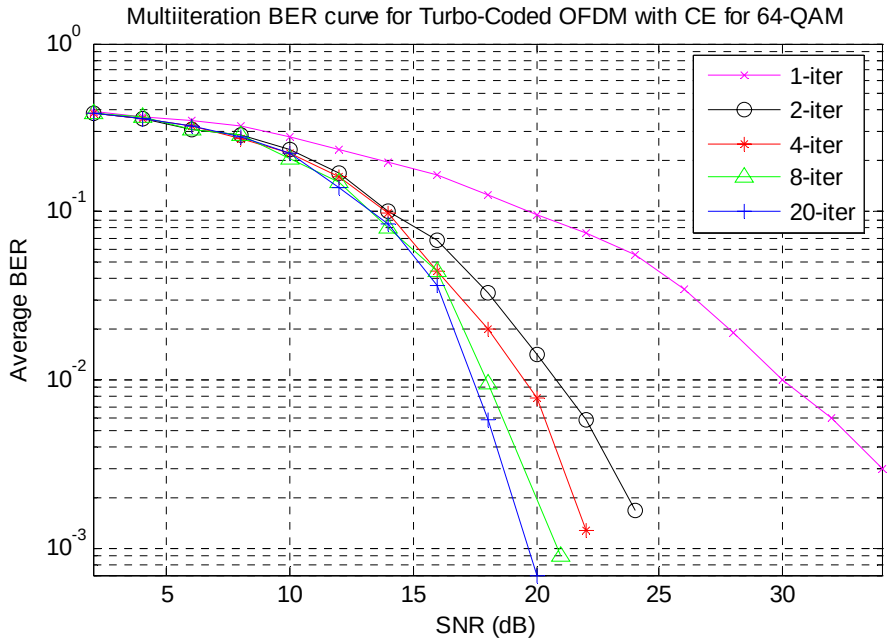

Figure 5.30: Comparison curve of Turbo-Coded OFDM with Channel Estimation for 16-QAM modulation for 1,2,4,8 and 20 iterations of MAP decoder in Rayleigh fading AWGN channel

BER curves for the proposed model of OFDM with 64-QAM are given below. OFDM symbol is comprised of 256 subcarriers and the size of the cyclic prefix is 64. The size of one OFDM Symbol is 1.5kbits and the size of one frame unit as depicted in figure 5.1 is 9Kbits (information data). 1/3 rate encoder is used at the transmitter side and the decoder at the receiver uses

MAP decoding algorithm. The BER performance of 64-QAM with different number of iterations of Turbo MAP decoder is shown below.

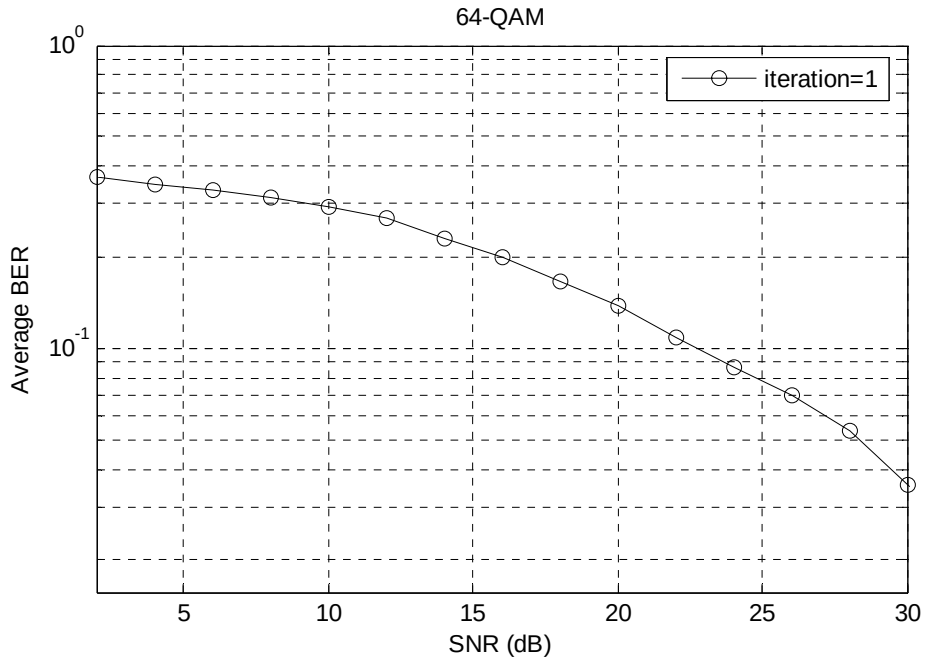

Figure 5.31: BER Curve of Turbo-Coded OFDM with Channel Estimation for 64-QAM modulation scheme on Rayleigh fading AWGN channel for single iteration of MAP Decoder

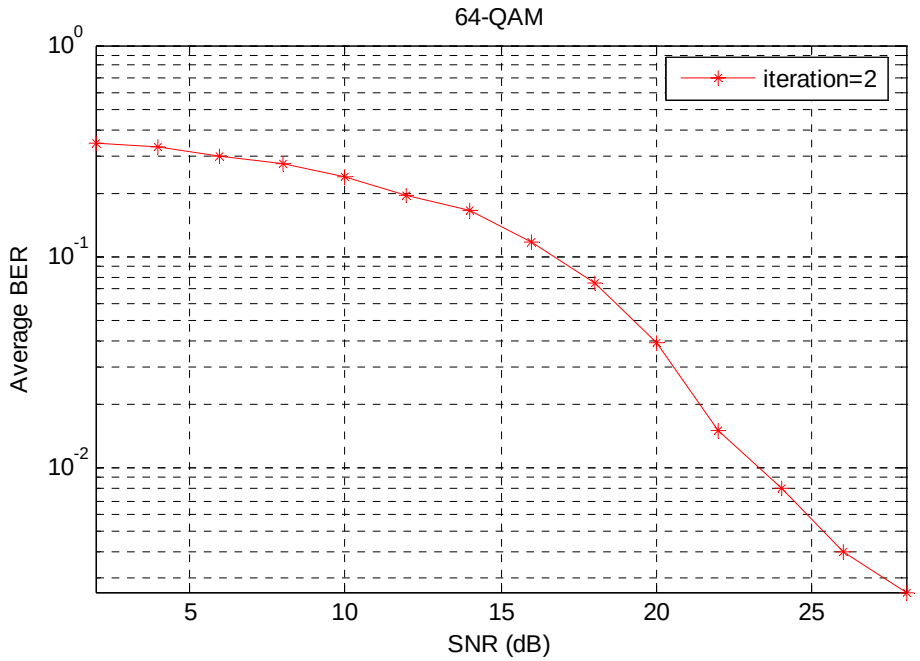

Figure 5.32: BER Curve of Turbo-Coded OFDM with Channel Estimation for 64-QAM modulation scheme on Rayleigh fading AWGN channel for 2 iterations of MAP Decoder

Figure 5.31 and 5.32 shows an improvement in the bit error rate of the system when the iteration is increases from 1 to 2. But the succeeding figures will show that the gain is very less when the number of iteration is increased to 4, 8 and then 20. It is because of the congested constellation mapping of the symbols which are 12.8571° apart for the squared constellation case for 64-QAM. It is depicted in figure 5.33, 5.34, 5.35 and then in the combine graph of figure 5.36 shown below.

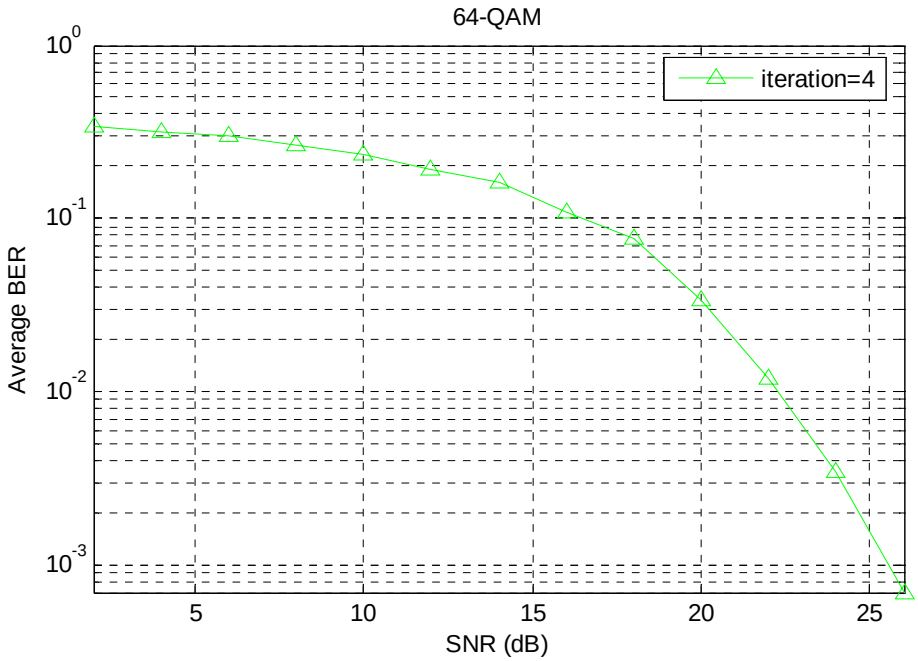

Figure 5.33: BER Curve of Turbo-Coded OFDM with Channel Estimation for 64-QAM modulation scheme on Rayleigh fading AWGN channel for 4 iterations of MAP Decoder

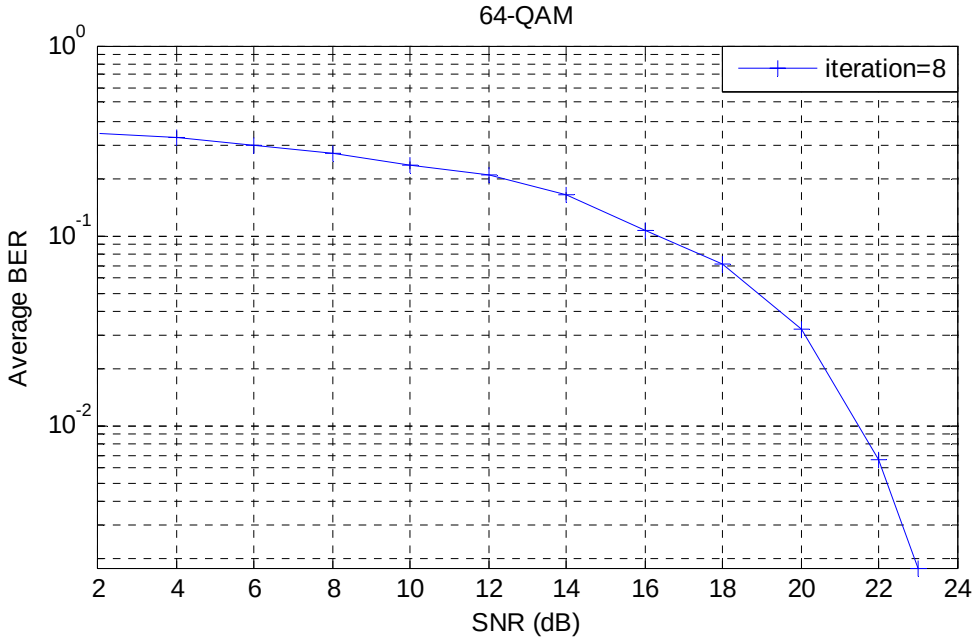

Figure 5.34: BER Curve of Turbo-Coded OFDM with Channel Estimation for 64-QAM modulation scheme on Rayleigh fading AWGN channel for 8 iterations of MAP Decoder

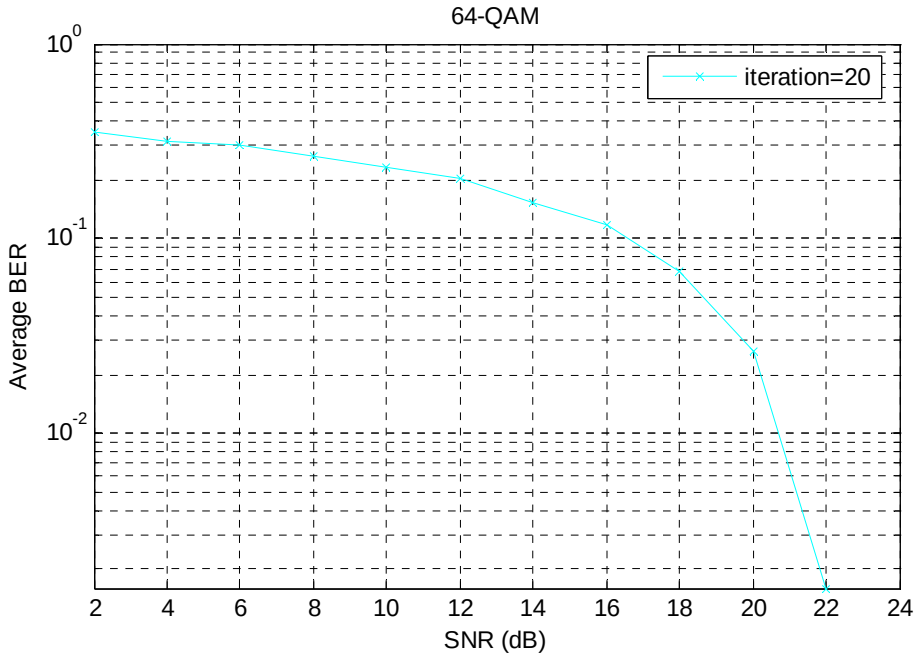

Figure 5.35: BER Curve of Turbo-Coded OFDM with Channel Estimation for 64-QAM modulation scheme on Rayleigh fading AWGN channel for 20 iterations of MAP Decoder

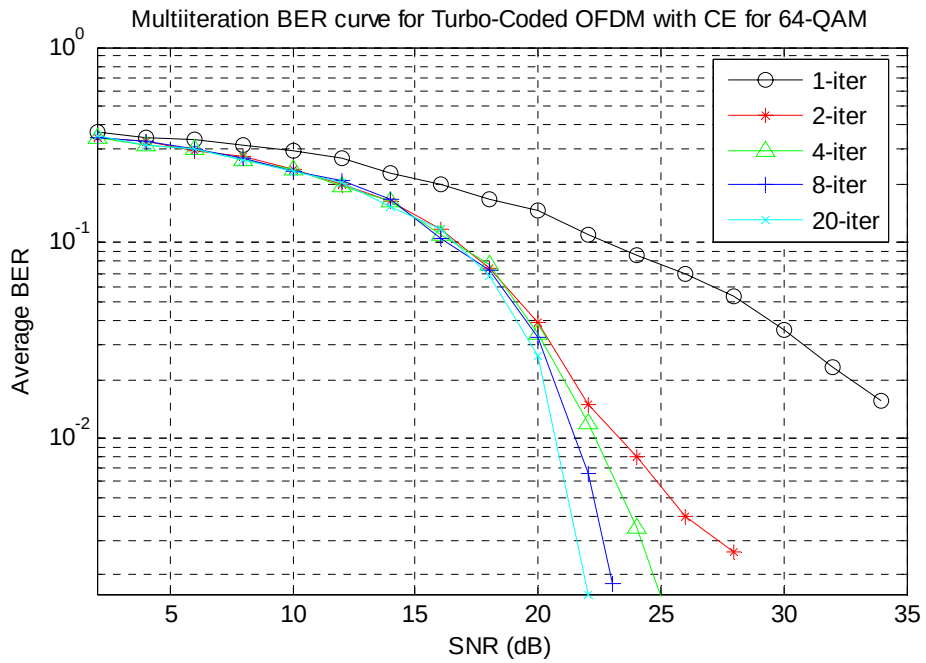

Figure 5.36: Comparison curve of Turbo-Coded OFDM with Channel Estimation for 64-QAM modulation for 1,2,4,8 and 20 iterations of MAP decoder in Rayleigh fading AWGN channel

The 20 iteration graph given in figure 5.35 when compared with the same in figure 5.12 shows a performance loss of almost 4dB due to the presence of the Rayleigh distributed fading in the channel through which the signal is passed. Communication parameters are the same in both the cases.

The multi-iteration graph shown in figure 5.36 shows practically, the theoretical inferences made from the start of the chapter. Figure 5.35 shows an SNR gain of almost 1 dB for a very high computational complexity and thus latency introduction into the system due to the addition of 12 extra iterations at the receiver end. That's the reason that for real-time services

which are delay sensitive though error tolerant to some extent, the number of iterations are kept small. For non-real time services, which are delay tolerant and error sensitive, the number of iterations is normally kept large. Therefore the choice of the number of iterations of MAP decoder is a critical factor for the system designers.

5.6 Comparison

We have compared our work with the work of Elnoubi [35] presented in MILCOM 2008 proceedings. Figure 5.37 shows the BER performance of the above referred work for uncoded and turbo-coded OFDM with comb-type channel estimation for 4 iterations of turbo decoder for QPSK modulation scheme.

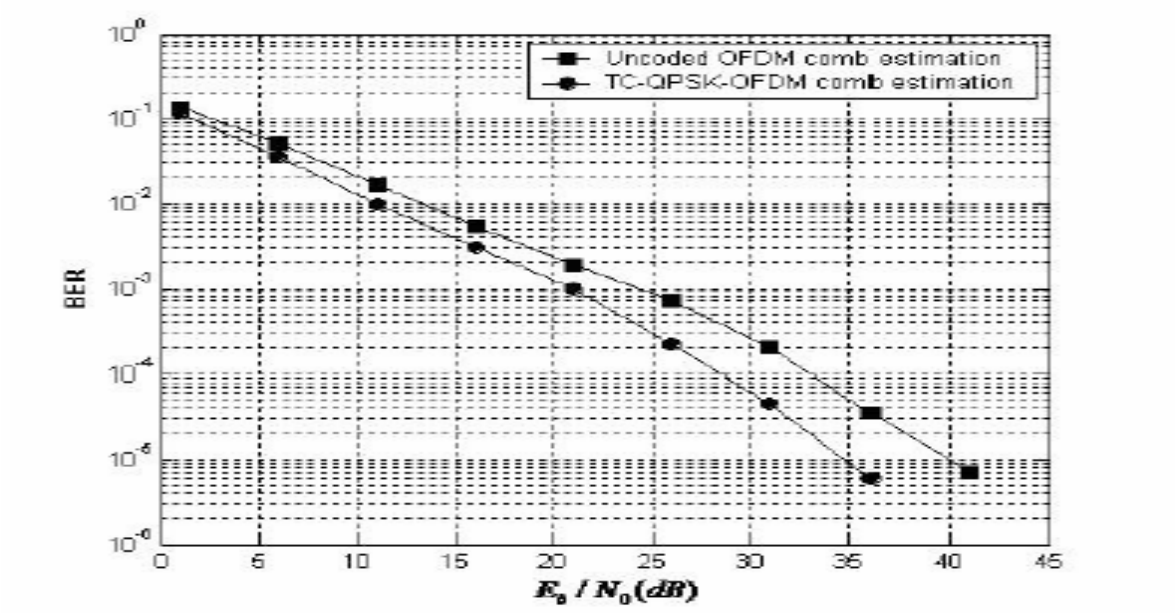

Figure 5 . BER of TC-QPSK-OFDM with comb pilot data in Rayleigh Fading Channel

Figure 5.37: Results of the above referred model for Turbo-coded OFDM system with comb type channel estimation for 4 iterations of Turbo MAP decoder[35]

For uncoded OFDM system with channel estimation, our work shown in (Figure 5.24) shows an SNR requirement of 22 dB for 10e-3 BER performance while the same performance is achieved at 24.5 dB in the referred work of Figure 5.36. This coding gain of 2.5 dB corresponds to the block-type channel estimation that I have used in my work against the comb-type channel estimation used in the referred comparison paper. Comb-type channel estimation adds an extra Interpolation step in the calculation of the channel estimation response which adds to the loss of performance. Contrarily, in block-type channel estimation the channel estimates are directly calculated from the pilot tones and no interpolation step is involved.

For the turbo-coded OFDM system, the proposed model shows a performance improvement of 3.1 dB (Figure 5.23) for 4 iterations when compared with the referred work of figure 5.36 for a BER performance of 10e-3. This improvement is for two reasons. Firstly, use of Block-type channel estimation and secondly 1/3 rate turbo codes have been used against ½ rate in the referred work of figure 5.37. The additional parity bits increases the coding gain at the expense of extra bandwidth utilization i.e. we gain an energy efficiency at the expense of bandwidth efficiency.

5.7 Conclusion

In this chapter performance of the proposed model of OFDM with Channel estimation and error correction using Turbo codes has been elaborated with the help of BER curves obtained through MATLAB simulation. The performance graphs have been obtained with/without the implementation of Turbo codes in the proposed system. The comparison shows the coding gain that is achieved due to the application of Turbo codes with different modulation schemes. Individual performance curves for different number of iterations of MAP decoder have also been shown and compared. These curves show that the performance of the system converges as the numbers of iterations are increased beyond a certain value. Any further increase in the number of iterations improves the coding gain very less at the expense of high computational complexity addition into the system.

Chapter-6

CONCLUSION AND FUTURE WORK

6.1 Conclusion

As discussed in section 2.2, OFDM is a technique that is used in the applications where the user is in search of high data rates. Whenever the system goes to high data rates the channel induced impairments in the data causes errors. In our work we have estimated and equalized the channel taps and have shown that the performance of the system has been much improved with this estimation and equalization algorithm. A BER of 10e-3 is promised to be achieved at affordable SNR by the application of presented algo. The channel estimation has been done by zero forcing technique that involves frequency-domain pilot-assisted block type channel estimation strategy and performance of the system has been discussed in Ch 5.

Alongwith this, by the integration of error correcting Turbo Codes, the performance of the system has further been improved. The combination of parallel concatenation and recursive decoding allows these codes to achieve much improved performance. The BER of the system has been dropped further down to the range of 10e-4 by the application of Turbo Codes. The proposed system has been passed through AWGN as well as Rayleigh fading channel and the performance of the system has been tested individually with

and without the Turbo codes. Alongwith this, the decoder has been implemented using MAP decoding algorithm based on the exchange of soft information between two component MAP decoders. As the numbers of iterations are increased the LLR of the decoder output diverges from its mean 0 towards +ive or –ive side to depict a 1 or 0 decoded bit.

6.2 Future Work

This thesis is focused on the combination of Turbo codes and Channel Estimation and equalization in OFDM environment. Though these two parameters of the system have been covered with sufficient details there are still a few areas that are to be explored yet.

First problem is the elimination of Peak to Average Power Ratio (PAPR) in OFDM. This problem tends to lose the information because of the expansion of the high peaks of data outside the active region of the amplifier at the transmitter and receiver. So the provision of PAPR problem solution in the proposed system can prove to be a good addition to our work.

Secondly, the work done by us is in SISO environment. If the same work is implemented in MIMO environment the proposed system will move more quickly towards the practical implementation with a system performance improvement because MIMO improves QOS if used for diversity gain and improves data rate if used for multiplexing.

7. Bibliography

[1] Yaobin Win & Florence Danilo-Lemoine, "A postfix synchronization method for OFDM and MIMO-OFDM systems", *in the WCNC 2008 proceedings,* pp:1-6, March 31,08 to April 3, 2008.

[2] Daniele Lo Iacono, Marco Ronchi, Luigi Della Torre, and Fabio Osnato, "MIMO-OFDM Physical Layer Real-Time Prototyping" *in WCNC 2008 proceedings,* pp:18-23, March 31,08 to April 3, 08.

[3] Ahmad R. S. Bahai, Burton R. Salatzburg, "*Multicarrier Digital Communications,Theory and applications of OFDM",* Kluwer Academic publishers, 1999.

[4] Ramjee Prasad*, "OFDM for wireless communication systems"*, Universal Personal Communication Series, 2004.

[5] Mosier, R. R., and R. G. Clabaugh, "Kineplex, a bandwidth efficient binary transmission system", *AIEE trans.,* Vol. 76, pp:723-728, Jan. 1958.

[6] Porter, G. C., "Error distribution and diversity performance of a frequency differential PSK HF, modem", *IEEE trans. on Comm.,* Vol., COM-16, pp:567-575, Aug. 1968.

[7] Zimmerman, M. S., and A. L. Kirsch, "The AN/GSC-10 (KATHRYN) variable rate data modem for HF radio", *IEEE trans. on Comm.,* Vol,. COM-15,pp:197-205, April 1967.

[8] "*Orthogonal Frequency Division Multiplexing,"* U.S. Patent No. 3,488,4555, filed November 14, 1966, issued January 6, 1970.

[9] S. Weinstein and P. Ebert, "Data transmission by frequency division multiplexing using the discrete Fourier transform", *IEEE trans. On Comm.,*Vol. COM-19, pp:628-634, October 1971.

[10] V.K. Shrivastava, S.L.Maskara, "Performance of OFDM with channel coding and CDM for WLAN applications", *proc. Of national conference in Comm. (NCC-04),* pp: 6-9, Feb, 2004.

[11] Won Gi Jeon, Kyung Hi Chang, Yong Soo Cho, "An equalization technique for orthogonal frequency-division multiplexing systems in time-variant multipath channels",*IEEE transactions on communications*, Vol.47, No. 1, pp27-32, Jan 1999.

[12] Pornpimon Chayratsami, Mark A. Wickert, "Channel Estimation and mitigation techniques for OFDM in a Doppler Spread Channel"*, in the IEEE GLOBECOM 2008 proceedings,* pp:1-5, Nov 30,08 to Dec 4, 2008.

[13] Charan Lingriton, "Inter-Symbol Interference (ISI) and Root-Raised Cosine filtering" *http://www.complextoreal.com*, March, 2009.

[14] Tiejun (Ronald) Wang, John G. Proakis, and James R. Zeidler, *"*Techniques for Suppression of Intercarrier Interference in OFDM Systems*", in IEEE WCNC 2005 proceedings,* Vol.01, pp:39-44, 13-17 March,05.

[15] Yao Xiao "OFDM modulation and Intercarrier interference cancellation"*,* MS (EE) dissertation, Univ. of Louisiana, 2003.

[16] Shannon C. E., "A Mathematical Theory of Communication", *Bell System Technical Journal,* vol. 27, pp. 379-423, July 1948, and pp. 623-656, October 1948.

[17] L. Hanzo, T. H. Liew, B. L. Yeap, "Turbo Coding, Turbo Equalization and Space-Time Coding for Transmission over Wireless Channels**"** *monograph* ,University of Southampton UK,1963.

[18] R. Hamming, "Error detecting and error correcting codes", *Bell System Technical Journal,* vol. 29, pp. 147.160, 1950.

[19] P. Elias, "Coding for noisy channels", *IRE Convention Record*, pt.4, pp. 37.47, 1955.

[20] J. Wozencraft, "Sequential decoding for reliable communication", *IRE Natl. Conv. Rec*., vol. 5, pt.2, pp. 11.25, 1957.

[21] J. Wozencraft and B. Reiffen, "Sequential Decoding", *Cambridge, MA,* USA: MIT Press, 1961.

[22] R. Fano, "A heuristic discussion of probabilistic coding",*IEEE Transactions on Information Theory*, vol. IT-9, pp. 64.74, April 1963.

[23] J. Massey,"Threshold Decoding". *Cambridge, MA,* USA: MIT Press, 1963.

[24] A.Viterbi,"Error bounds for convolutional codes and an asymptotically optimum decoding algorithm*", IEEE Transactions on Information Theory,* vol. IT-13, pp. 260.269, April 1967.

[25] G. Forney,"The Viterbi algorithm", *Proceedings of the IEEE*, vol. 61, pp. 268.278, March 1973.

[26] J. H. Chen, "High-quality 16 kb/s speech coding with a one-way delay less than 2 ms", *in Proceedings of International Conference on Acoustics, Speech, and Signal Processing,* ICASSP.90, vol. 1, (Albuquerque, New Mexico, USA), pp. 453.456, IEEE, 3.6 April 1990.

[27] Berrou C., Glavieux A., Thitimajshima P, "Near Shannon Limit Error-Correcting Coding and Decoding: Turbocodes (1)", *in IEEE Int. Conf. on Comm. ICC'93*, pp. 1064-1071, vol. 2, 23-26 May 1993.

[28] Hamid R. Sadjadpour, "Maximum *a posteriori* decoding algorithm for Turbo Codes",*in proceedings of SPIE,* Vol. 4045, 2000

[29] Muhammad Arif, N. M. Sheikh, Asrar U.H. Sheikh "A novel design of deterministic interleaver for turbo codes", *IEEE Int. Conf. on Elec. Engg., ICEE '07*, pp: 1-5, April, 07.

[30] Valery Ramon,"Performance analysis of turbo equalization with channel estimation", PhD dissertation, Univrsity College London(UCL), 2007.

[31] Meng-Han Hsieh, Che-Ho Wei, "Channel estimation for OFDM Systems based on comb-type pilot arrangement in frequency selective fading channel", *IEEE transactions on consumer electronics*, Vol. 44, No. 1, pp:217-225,February 1998.

[32] Lucky. R.W,"Automatic equalization for digital communication", *Bell System technical journal*, vol 44, pp.547-588, 1965.

[33] Sergio Benedetto, Ezio Biglieri, *"Principles of Digital transmission:with wireless applications",*Springer, 1 edition, June 1999.

[34] Giovanni E. Corazza *"Digital Satellite Communication"*, Springer Science+Business media, pp-244, NY.2007.

[35] Elnoubi. S *et al,* "Performance of OFDM system with comb-type channel estimation in Rayleigh fading environment", *in the IEEE MILCOM 2008 proceedings*